Ataxin-2 and huntingtin interact with endophilin-A complexes to function in plastin-associated pathways

Markus Ralser[1],[†], Ute Nonhoff[1],[†], Mario Albrecht[2], Thomas Lengauer[2], Erich E. Wanker[3], Hans Lehrach[1] and Sylvia Krobitsch[1],*

[1]Max Planck Institute for Molecular Genetics, Ihnestrasse 73, 14195 Berlin, Germany, [2]Max Planck Institute for Informatics, Stuhlsatzenhausweg 85, 66123 Saarbrücken, Germany and [3]Max Delbrueck Center for Molecular Medicine, Robert-Roessle-Strasse 10, 13092 Berlin, Germany

Spinocerebellar ataxia type 2 is an inherited neurodegenerative disorder that is caused by an expanded tri-nucleotide repeat in the *SCA2* gene, encoding a polyglutamine stretch in the gene product ataxin-2. Although evidence has been provided that ataxin-2 is involved in RNA metabolism, the physiological function of ataxin-2 remains unclear. Here, we demonstrate that ataxin-2 interacts with two members of the endophilin family, endophilin-A1 and endophilin-A3. To elucidate the physiological implications of these interactions, we exploited yeast as a model system and discovered that expression of ataxin-2 as well as both endophilin proteins is toxic for yeast lacking the *SAC6* gene product fimbrin, a protein involved in actin filament organization and endocytotic processes. Intriguingly, expression of huntingtin, another polyglutamine protein interacting with endophilin-A3, was also toxic in Δsac6 yeast. These effects can be suppressed by simultaneous expression of one of the two human fimbrin orthologs, L- or T-plastin. Moreover, we have discovered that ataxin-2 associates with L- and T-plastin and that overexpression of ataxin-2 leads to accumulation of T-plastin in mammalian cells. Thus, our findings suggest an interplay between ataxin-2, endophilin proteins and huntingtin in plastin-associated cellular pathways.

INTRODUCTION

Spinocerebellar ataxia type 2 (SCA2) is an autosomal dominant cerebellar ataxia, which is characterized by a severe loss of neuronal cells leading to uncoordinated gait, slow saccadic eye movement, peripheral neuropathy, intellectual impairment and dementia (reviewed in 1). SCA2 occurs with a frequency of 10–15% within the autosomal dominant cerebellar ataxias (2). However, the prevalence of SCA2 varies between countries and is fairly widespread in the UK and South Italy with ∼47% of all autosomal dominant spinocerebellar ataxia cases diagnosed as SCA2 followed by India with 44% (3,4). The gene causative of SCA2 was discovered in 1996 and is transcribed in neuronal as well as non-neuronal tissues (5–7). Although the majority of normal alleles contain a stretch of 22 CAG codons that is commonly interrupted by two CAA codons, disease alleles are characterized

by an extended, generally uninterrupted stretch of 32 or more CAG codons (5–9). Consequently, SCA2 has been classified into the family of polyglutamine disorders, which includes Huntington's disease, spinobulbar muscular atrophy, dentatorubral pallidoluysian atrophy and spinocerebellar ataxias 1, 3, 6, 7 and 17 (1,10–15).

In most polyglutamine disorders, intranuclear and/or cytoplasmic aggregates have been observed in the degenerating neurons of the respective brain regions, although the relevant polyglutamine proteins are ubiquitously expressed (discussed in 16 and 17). However, the formation of nuclear/cytoplasmic inclusions does not obligatorily correlate with the pathology in SCA2; aggregates were only rarely detected in the cerebellar lesions in mouse and human, although aggregates have been observed in a small subset of neurons in other affected brain regions (18–20). Instead, immunohistological and biochemical studies demonstrated that the expression of the *SCA2*

---

gene product, ataxin-2 (ATX2), is significantly higher in brains of SCA2 patients when compared with brains of healthy individuals indicating that an increase in intracellular ATX2 concentration may correlate with disease progression (18,21).

Yet the physiological function of ATX2, which is located in the cytoplasm and found to localize to the trans-Golgi network (22), remains unclear. However, it has been proposed that ATX2 might function in RNA metabolism. Shibata *et al.* (23) discovered by yeast-two-hybrid analyses an interaction between ATX2 and A2BP1 (ATX2 binding protein 1), which contains an RNA-recognition motif frequently found in RNA-binding proteins (24). In addition, ATX2 interacts with the cytoplasmic poly(A)-binding protein (PABP) (25) that functions in translation initiation and mRNA decay regulation and forms part of the so-called stress granules (26,27). These granules arise in mammalian cells because of environmental stresses such as oxidative stress or UV irradiation and may well represent sites for degradation or storage of untranslated mRNAs (27). Immunofluorescence studies have demonstrated that ATX2 is a component of stress granules as well (25). Nevertheless, further investigations into the cellular role of ATX2 are required to explore and to elucidate the cellular networking of ATX2.

RESULTS

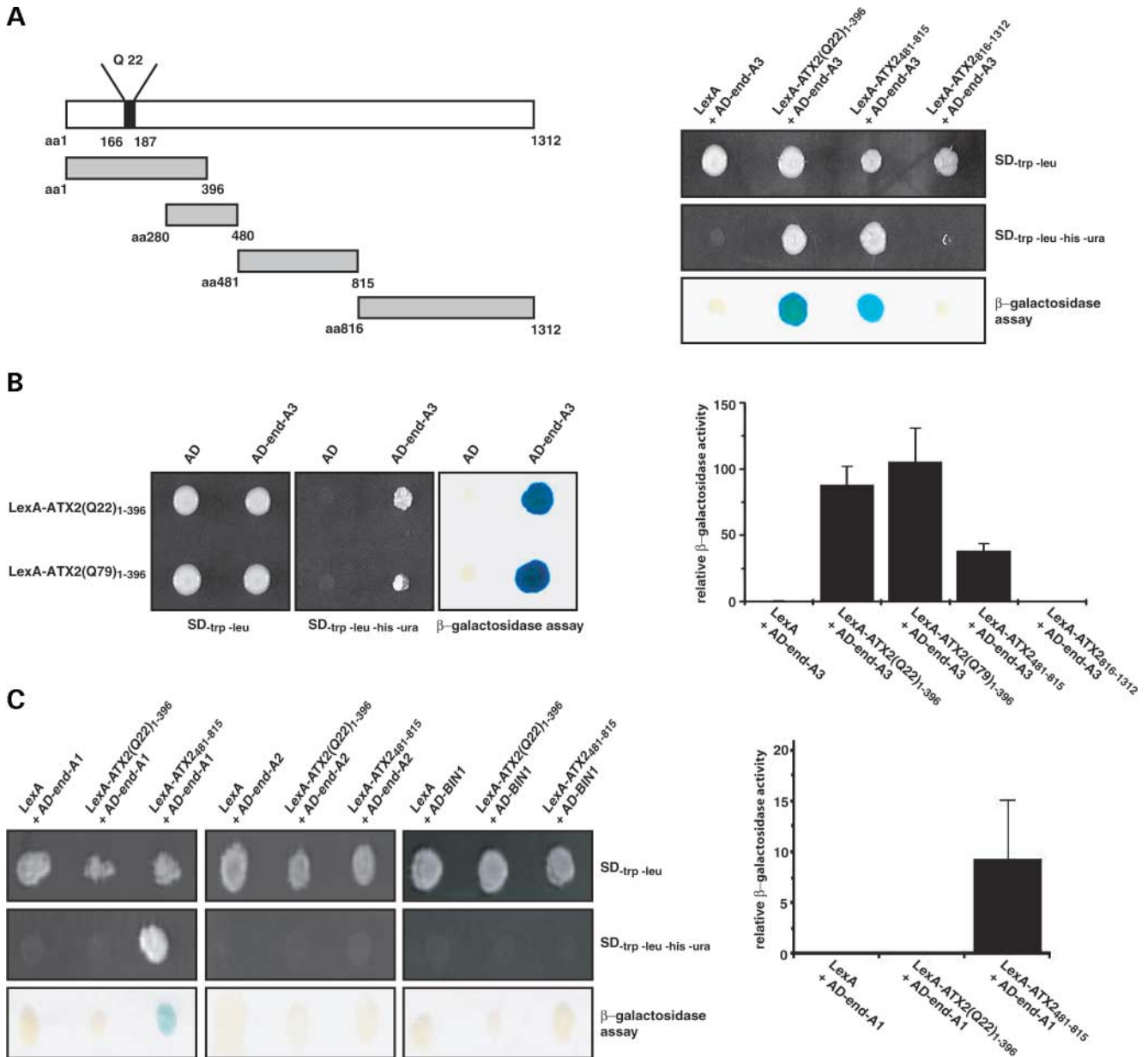### ATX2 interacts with members of the endophilin-A family

To perform a comprehensive yeast-two-hybrid analysis, we have generated constructs encoding four different LexA−ATX2 fusion proteins, which together cover the entire ATX2 protein with a molecular mass of 140 000 (5−7,19). The ATX2 regions that have been selected are shown schematically in Figure 1A (left panel). We chose a N-terminal region of ATX2 consisting of amino acids 1−396 because an N-terminal protein fragment of similar size was found in human and mouse brains (18,19,21). Furthermore, an acidic region of ATX2 encompassing amino acids 280−480 was subcloned (19). The C-terminal fragment of ATX2 (amino acids 816−1312) applied in this study was selected, because it has been successfully used for the isolation of interacting partner proteins in earlier studies (23,25). Finally, to cover the whole ATX2 protein, we have generated an additional fusion construct encoding amino acids 481−815 of ATX2.

In the initial step, we tested whether the different ATX2 bait proteins *per se* might activate the reporter genes as described in Materials and Methods. We observed that the expression of fusion protein LexA−ATX2$_{280−480}$ by itself activated the reporter genes *URA3, HIS3* and *LacZ* (data not shown), and consequently, it was not used for further yeast-two-hybrid screens. Next, yeast cells expressing the fusion proteins LexA−ATX2(Q22)$_{1−396}$, LexA−ATX2$_{481−815}$ or LexA−ATX2$_{816−1312}$ were mated with an array of 5760 prey strains. Diploid yeast clones were selected and analyzed for activity of the reporter genes. Once activation of the reporter genes was observed, mating between the respective bait and prey clones was performed again. As outcome of this procedure, we have isolated, for each ATX2 bait protein, one potential interacting prey protein.

To verify the results from the mating screen, we co-transformed the relevant bait and prey constructs in the haploid yeast strain L40ccua. We found that the potential interaction observed for bait protein LexA−ATX2$_{816−1312}$ could not be confirmed in this background (data not shown). However, in the case of the bait proteins LexA−ATX2(Q22)$_{1−396}$ and LexA−ATX2$_{481−815}$, the putative interaction could be confirmed as indicated by the activity of all three reporter genes. Interestingly, a subsequent sequence analysis identified that both prey constructs encoded the protein endophilin-A3 (SH3GL3, SH3P13, CNSA3) (Fig. 1A, right panel). To verify that the interaction between ATX2 and endophilin-A3 is specific, yeast co-expressing fusion proteins AD-endophilin-A3 (AD-end-A3) and the proteins LexA or LexA−ATX2$_{816−1312}$ were included in our yeast-two-hybrid analysis. We discovered that in both cases yeast did not exhibit activity of the reporter genes. Additionally, ataxin-3, a polyglutamine protein implicated in spinocerebellar ataxia 3, was included as an unrelated bait protein. No interaction between ataxin-3 and AD-end-A3 was observed in the yeast-two-hybrid system (data not shown), demonstrating that the observed interaction between ATX2 and endophilin-A3 is specific.

As endophilin-A3 binds to the N-terminal region of ATX2, we examined in the next step whether this interaction is affected by an expanded polyglutamine stretch. Therefore, yeast clones expressing LexA−ATX2(Q22)$_{1−396}$/AD-end-A3 or LexA−ATX2(Q79)$_{1−396}$/AD-end-A3 were spotted onto selective media to analyze the activity of the reporter genes. No growth difference between yeast co-expressing LexA−ATX2(Q22)$_{1−396}$/AD-end-A3 and yeast co-expressing LexA−ATX2(Q79)$_{1−396}$/AD-end-A3 was observed (Fig. 1B, left panel). A significant difference in the relative activity of the *LacZ* reporter gene as analyzed by membrane-based or liquid β-galactosidase assays was also not detected (Fig. 1B, left and right panels). Thus, an expanded polyglutamine stretch in ATX2 did not appear to affect the interaction with endophilin-A3 in the yeast-two-hybrid system.

Endophilin-A3 belongs to a unique SH3 protein family that includes the two highly homologous paralogs endophilin-A1 (SH3GL2, SH3P4, CNSA2) and endophilin-A2 (SH3GL1, SH3P8, CNSA1) (28). Therefore, we investigated in a directed yeast-two-hybrid analysis whether these proteins also associate with ATX2. We discovered that yeast cells co-expressing the fusion proteins LexA−ATX2$_{481−815}$ and AD-end-A1 exhibited activity of all three reporter genes indicating a potential interaction (Fig. 1C), whereas in yeast cells co-expressing LexA−ATX2(Q22)$_{1−396}$ and AD-end-A1 no activity of the reporter genes was observed. This indicates that endophilin-A1 associates with the central ATX2 region (amino acids 481−815) but not with the N-terminal region (amino acids 1−396) which contains the polyglutamine stretch. No activity of the reporter genes was observed in yeast cells co-expressing the ATX2 fragments with AD-end-A2 or the control prey protein AD-BIN1 (amphiphysin II, SH3P9, AMPHL), which has a high similarity to endophilin proteins (29). In summary, these results indicate that ATX2 interacts with two members of the endophilin family, endophilin-A1 and endophilin-A3, but not with endophilin-A2. This is fairly interesting in the light that, in particular, the

Figure 1. ATX2 interacts with two members of the endophilin family. (**A**) Left panel: schematic representation of ATX2 and its regions (gray boxes) applied in the yeast-two-hybrid studies. The black box indicates the polyglutamine stretch of 22 glutamines. Right panel: to verify the interaction between ATX2 and endophilin-A3 observed in the yeast-two-hybrid-array screen, the haploid yeast strain L40ccua was co-transformed with the respective plasmids encoding LexA/AD-end-A3, LexA−ATX2(Q22)$_{1-396}$/AD-end-A3, LexA−ATX2$_{481-815}$/AD-end-A3 or LexA−ATX2$_{816-1312}$/AD-end-A3, and transformants were spotted onto selective media or on a membrane to analyze the activity of the three reporter genes *URA3, HIS3* and *LacZ*. (**B**) Left panel: yeast cells co-expressing fusion proteins LexA−ATX2(Q22)$_{1-396}$ and AD-end-A3 or LexA−ATX2(Q79)$_{1-396}$ and AD-end-A3 were analyzed for activity of the reporter genes on selective SD medium and by a membrane-based β-galactosidase assay. As controls, yeast was transformed with the respective ATX2 bait vector and the empty prey vector. Right panel: liquid β-galactosidase assay. Yeast cells co-expressing proteins AD-end-A3 together with LexA, LexA−ATX2(Q22)$_{1-396}$, LexA−ATX2(Q79)$_{1-396}$, LexA−ATX2$_{481-815}$ or LexA−ATX2$_{816-1312}$ were tested for the relative β-galactosidase activity. For the calculation of the standard deviation, four yeast clones of each transformation were used for measurements, and the Nalimov method was applied to exclude statistical outliers. (**C**) Left panel: directed yeast-two-hybrid analysis. Yeast was co-transformed with plasmids encoding LexA−ATX2(Q22)$_{1-396}$ or LexA−ATX2$_{481-815}$ and the relevant prey plasmids encoding fusion proteins AD-end-A1, AD-end-A2 or AD-BIN1. The respective transformants were tested for activation of the three reporter genes. Right panel: liquid β-galactosidase assay was performed as described earlier.

SH3 domains of endophilin-A1 and endophilin-A3 have a closer homology to each other than to endophilin-A2 (28). The sequence identities of the respective SH3 domains are 90% for endophilin-A1/A3 in contrast to 83% and 79% for endophilin-A1/A2 and endophilin-A2/A3, respectively. In comparison, all full-length sequence identities are very similar with 68% for endophilin-A1/A3 and 71% and 67% for endophilin-A1/A2 and endophilin-A2/A3, respectively.

Finally, to corroborate our results from the yeast-two-hybrid analyses, we investigated whether the interaction between ATX2 and endophilin-A1 or endophilin-A3 occurs in mammalian cells. Therefore, we transiently transfected COS-1 cells with expression plasmids encoding the respective cMYC-tagged ATX2 regions, cMYC-ATX2(Q22)$_{1-396}$ or cMYC-ATX2$_{481-815}$ and FLAG-tagged full-length endophilin-A1 (FLAG-end-A1) or endophilin-A3 (FLAG-end-A3). Our co-immunoprecipitation experiments demonstrated that FLAG-end-A3 precipitated with cMYC-ATX2(Q22)$_{1-396}$ protein using an antibody directed against the cMYC-tag (Fig. 2A, left panel). In addition, FLAG-end-A1 and FLAG-end-A3 were precipitated with cMYC-ATX2$_{481-815}$ protein (Fig. 2A, right panel). No endophilin proteins were precipitated in control lysates.

In addition, co-localization studies staining endogenous proteins in HEK293 and SH-SY5Y cells showed that both endophilin proteins and ATX2 are present in the cytoplasm (Fig. 2B). Besides, ATX2 and endophilin-A1 or endophilin-A3 do co-localize to some extent in the axons of differentiated SH-SY5Y cells (Fig. 2B (i−k) and (t−v)).

Interaction between ATX2 and the endophilin proteins depends on their SH3 domains and two specific proline-rich binding motifs within ATX2
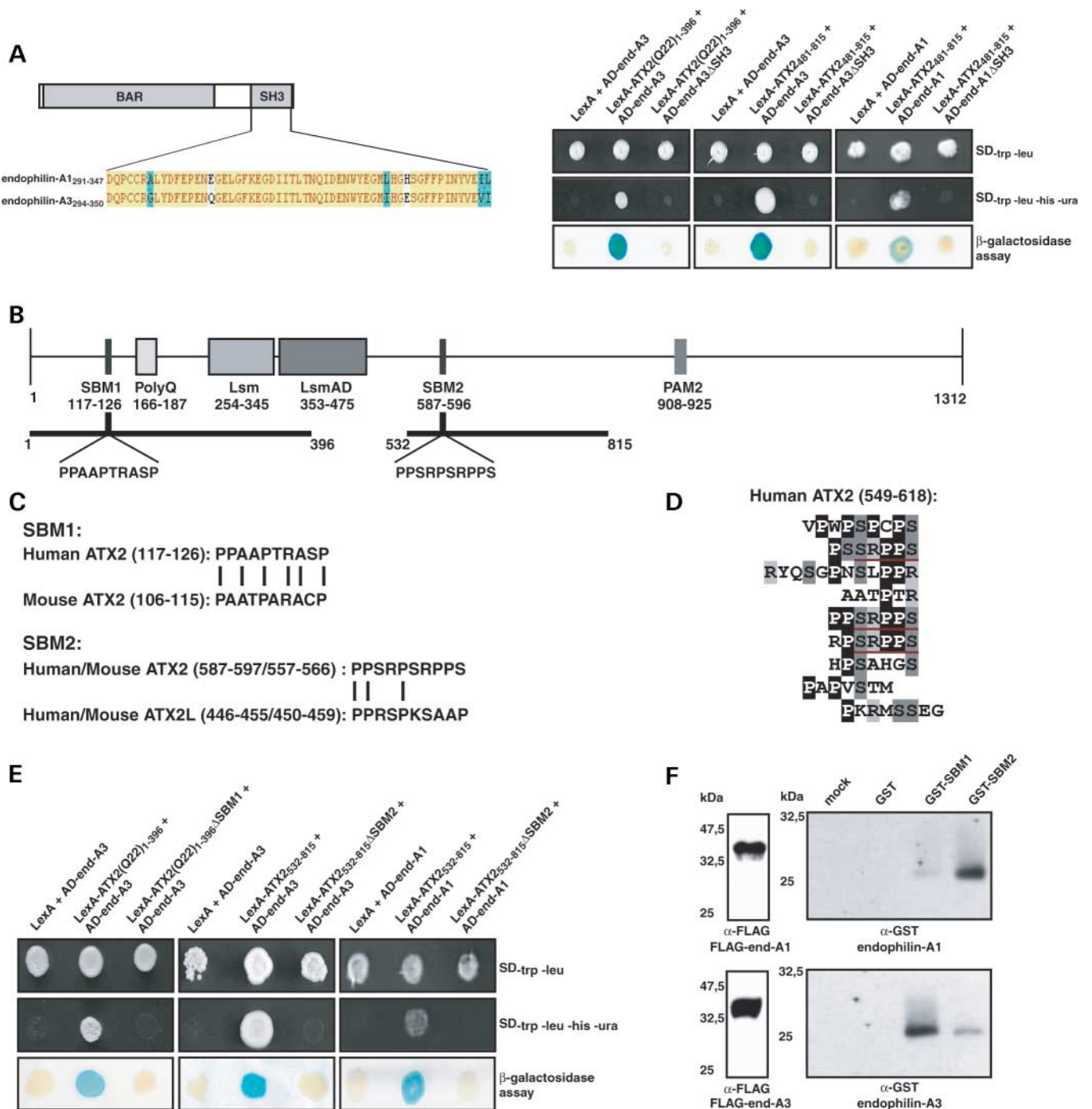
To further characterize the interaction between ATX2 and the endophilin proteins, we wanted to identify the regions responsible for binding. Endophilin proteins are composed of an N-terminal BAR domain and a C-terminal SH3 domain that commonly binds proline-rich regions within proteins (Fig. 3A, left panel) (30). First, we analyzed whether the interaction between ATX2 and both endophilin proteins depends on the C-terminal SH3 domain. Yeast-two-hybrid constructs encoding the fusion proteins AD-end-A1 or AD-end-A3 (31) without the SH3 domain were co-expressed with LexA−ATX2(Q22)$_{1-396}$ or LexA−ATX2$_{481-815}$, and the activity of the three reporter genes *URA3, HIS3* and *LacZ* was monitored (Fig. 3A, right panel). We observed that in yeast cells co-expressing LexA−ATX2(Q22)$_{1-396}$ or LexA−ATX2$_{481-815}$ with AD-end-A1 or AD-end-A3 lacking the SH3 domain, transcription of the reporter genes did not occur. Thus, the C-terminal SH3 domain of endophilin-A1 and endophilin-A3 is required for the interaction with ATX2.

Secondly, because proline-rich protein regions that adopt a helical polyproline type II conformation are accountable for binding the SH3 domain of the different endophilin proteins (30,32), we searched for such regions within ATX2 using bioinformatics methods. Both methods, iSPOT and Scansite, consistently detected two potential SH3 binding motifs (SBM1 and SBM2) for SH3 domain proteins including endophilins (Fig. 3B). Both SH3 binding sites received top-ranked confidence scores that indicate a very high reliability for functional relevance: 0.86/0.92 from iSPOT (best 1.0, worst 0.0) and 0.40/0.36 from Scansite (best 0.0, worst $+\infty$) for SBM1/SBM2. In addition, the ELM online service reported that SBM1 and SBM2 are the only two SH3 binding peptides in ATX2, which belong to class II characterized by the consensus motif PxxPxR/S (33). This class commonly contains proline-rich peptides that are experimentally observed to
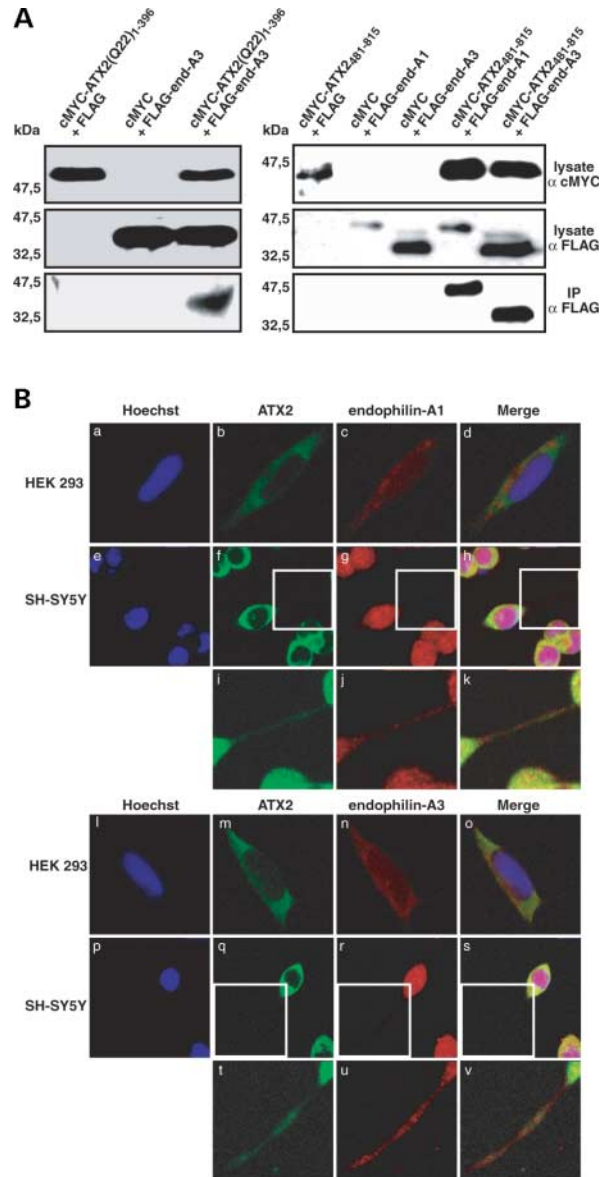
Figure 2. Interaction between ATX2 and endophilin-A1/endophilin-A3 occurs in mammalian cell lines. (**A**) Lysates have been prepared from COS-1 cells expressing cMYC-tagged ATX2 regions and FLAG-tagged endophilins or the respective controls. Expression of proteins has been analyzed by immunoblotting using α-cMYC or α-FLAG antibody (upper panels). For co-immunoprecipitation experiments 100−130 μg of each lysate was used and incubated with α-cMYC antibody. Precipitated proteins were visualized by immunoblotting using α-FLAG antibody (lower panels). (**B**) Co-localization of endogenous ATX2 and endophilin-A1 (a−d) or ATX2 and endophilin-A3 (l−o) in HEK 293 cells, or in differentiated SH-SY5Y cells (e−k) and (p−v). White boxes in (f−h) and (q−s) indicate enlargements of axon-like structures of SH-SY5Y cells, which are shown in pictures (i−k) and (t−v). For enlarged pictures, z-stacks of the lower area were used to clearly visualize the axon-like structures.

bind SH3 domains of endophilins (30,33). Further analyses revealed that SBM1 of human ATX2 is strongly conserved in mouse ATX2, and SBM2 is even the same in human and mouse orthologs (Fig. 3C). Prolines that are generally essential for class II SH3 domain binding peptides are mostly identical

Figure 3. Characterization of the interaction between ATX2 and endophilin-A1/endophilin-A3. (**A**) Left panel: schematic illustration of endophilin proteins and sequence alignment of the SH3 domains of endophilin-A1 and endophilin-A3. The BAR domain and SH3 domain are marked in gray. Sequence highlighted in yellow represents identical amino acids, whereas blue areas indicate physiochemical similarity of amino acid types. Right panel: yeast cells co-expressing the corresponding ATX2 bait and endophilin prey proteins with or without the SH3 domain were spotted onto selective media or on membrane for analyzing the activity of the reporter genes. (**B**) Domain architecture of ATX2. Gray boxes indicate the putative RNA-binding Lsm domain, the Lsm-associated domain LsmAD, the PABP-interacting motif PAM2 and the polyQ stretch. The two proline-rich SH3 domain binding motifs, SBM1 and SBM2, and their amino acid composition are shown additionally. The thick black lines represent ATX2 regions that have been chosen for the yeast-two-hybrid studies described in (E). (**C**) SBM1 sequences in human and mouse ATX2 as well as SBM2 sequences in human and mouse ATX2 and ATX2L paralogs. (**D**) Similar sequence repeats including SBM2 found in human ATX2. Three identical SRPPS motifs are underlined in red. Prolines, serines and arginines that are frequently conserved are highlighted. (**E**) Yeast co-expressing the relevant ATX2 regions (with or without SBM1 or SBM2) and endophilin-A1/endophilin-A3 were analyzed for reporter gene activity. (**F**) Lysates of COS-1 cells overexpressing FLAG-tagged endophilin-A1 or FLAG-tagged endophilin-A3 were incubated with purified GST or with fusion proteins GST–SBM1 or GST–SBM2 and cross-linked. Co-immunoprecipitation experiments were performed using a α-FLAG antibody. Precipitates and lysates were analyzed by immunoblotting using an α-GST antibody or an antibody directed against the FLAG-tag.

in human and mouse ATX2. Interestingly, SBM2 lies within a sequence region that contains similar sequence repeats (Fig. 3D) and is missing in two observed splice variants of mouse ATX2 (34). Because ATX2, as well as ataxin-2-like/related paralogs consist of mainly unstructured regions (35) containing many proline-rich sequence stretches, additional protein interactions with ATX2 may be mediated by domains recognizing such peptides (32,36). For instance, the ATX2 paralog ATX2L contains a proline-rich motif similar to that of SBM2 (Fig. 3C). SBM1 is located near the poly-glutamine stretch, whereas SBM2 lies in the middle region of ATX2 subsequent to the Lsm and LsmAD domains, but before the PABP-interacting motif PAM2 (Fig. 3B) (37). Noticeably, the sequence motifs SBM1 and SBM2 are part of the ATX2 regions that have been initially identified in our yeast-two-hybrid screen (Figs 1A and 3B). To experimentally verify the requirement of these motifs for binding, we have generated constructs that encode fusion proteins lacking the relevant regions, termed $LexA-ATX2(Q22)_{1-396}\Delta SBM1$ and $LexA-ATX2_{532-815}\Delta SBM2$ (Fig. 3E). The yeast-two-hybrid analysis showed that yeast cells co-expressing $LexA-ATX2(Q22)_{1-396}\Delta SBM1/AD-end-A3$, $LexA-ATX2_{532-815}\Delta SBM2/AD-end-A3$ or $LexA-ATX2_{532-815}\Delta SBM2/AD-end-A1$ did not exhibit activity of the reporter genes demonstrating that SBM1 and SBM2 binding motifs are essential for the interaction with the SH3 domain in endophilin-A1 and endophilin-A3.

Furthermore, we confirmed that both sequence motifs are responsible for the interaction performing an *in vitro* binding assay. To this end, expression plasmids encoding glutathione *S*-transferase (GST) fusion proteins for SBM1 and SBM2 were generated separately and proteins were purified. Subsequently, pure GST, GST–SBM1 and GST–SBM2 proteins were incubated with the identical lysate of COS-1 cells containing either recombinant FLAG-tagged endophilin-A1 or FLAG-tagged endophilin-A3. After cross-linking, the different lysate samples were incubated with an antibody directed against the FLAG-tag and co-immunoprecipitation experiments were performed. Precipitates were visualized by immunoblotting using an antibody directed against GST. As shown in Figure 3F, both proteins GST–SBM1 and GST–SBM2 were precipitated with an antibody directed against the FLAG-tag, demonstrating that these binding motifs are important for the interaction of ATX2 and endophilin-A3. Additionally, GST–SBM2 protein was precipitated with an antibody directed against FLAG-tagged endophilin-A1. Thus, these findings demonstrate that both motifs, SBM1 and SBM2, of ATX2 bind to endophilin proteins. However, we also observed that a minimal amount of GST–SBM1 was precipitated with endophilin-A1 protein. This finding seems to contrast our yeast-two-hybrid results (Fig. 1C, left panel), because an interaction between the N-terminal region of ATX2 (containing SBM1) and endophilin-A1 has not been detected. However, the precipitation of a small amount of SBM1 with endophilin-A1 from mammalian cell lysate could be based on complex formation of endophilin proteins, because homodimer as well as heterodimer formation has been observed for endophilin-A1 and endophilin-A2 proteins (38). Therefore, we investigated whether endophilin-A3 protein also interacts with the other endophilin-A members by applying a directed yeast-two-hybrid analysis. Yeast cells co-expressing LexA-end-A1/AD-end-A1, LexA-end-A1/AD-end-A2 or LexA-end-A1/AD-end-A3 exhibited growth on selective media indicating activation of the reporter genes (Fig. 4A). Furthermore, transcription of reporter genes was also observed in yeast expressing LexA-end-A2 or LexA-end-A3 in combination with AD-end-A1, AD-end-A2 and AD-end-A3. Thus, our yeast-two-hybrid analysis clearly showed that endophilin-A proteins interact with each other.

To confirm these observations in another experimental system, we investigated the interplay of endophilin proteins in mammalian cells performing co-immunoprecipitation experiments. COS-1 cells have been transiently transfected with constructs encoding the different endophilin proteins in a HA- or FLAG-tagged version. After incubating the cells for 3 days at 37°C to allow expression of proteins, cell lysates were prepared. Then, the cell extracts were mixed and incubated for 1 h at 4°C to allow the formation of homologous and heterologous endophilin complexes. Subsequently, co-immunoprecipitation experiments were performed as described in Materials and Methods. As Figure 4B shows, FLAG-end-A1 was precipitated from a lysate mixture containing HA-end-A1 using an antibody directed against the HA-tag (b), demonstrating the formation of a homologous complex as reported earlier (38). In addition, HA-end-A3 was precipitated from a lysate mixture containing FLAG-end-A1 protein using an antibody directed against the FLAG-tag (Fig. 4B(c)), indicating that a heterologous complex between endophilin-A3 and endophilin-A1 assembles in mammalian cells. We also showed that FLAG-end-A2 and FLAG-end-A3 was precipitated from a lysate mixture containing HA-end-A3 using an antibody directed against the HA-tag (Fig. 4B(d and e)). Thus, our results demonstrate that endophilin-A proteins form complexes with each other in mammalian cells.

ATX2 and huntingtin compete for binding to endophilin-A3 in the yeast-two-hybrid system

After characterizing the interaction between ATX2 and the endophilin proteins, we investigated the physiological significance of this interaction. Intriguingly, previous studies demonstrated that endophilin-A3 interacts with the huntingtin exon 1 (httex1) protein (31), another polyglutamine protein, in which an expansion of the polyglutamine stretch causes Huntington's disease (39). Equivalent to our results, the interaction between httex1 and endophilin-A3 depends on the C-terminal SH3 domain of endophilin-A3 and a proline-rich region within the first exon of huntingtin, which is close to the polyglutamine stretch. This proline-rich region is essential because its loss prevents interaction between endophilin-A3 and httex1 (31). Accordingly, we examined whether interplay takes place between these three proteins, because this could provide valuable information about the cellular context ATX2 is involved in. For this purpose, we decided to explore at first whether ATX2 and httex1 do compete for binding to endophilin-A3. Recently, we have generated a yeast-two-hybrid strain, namely L40KMX, that can be utilized to investigate competitive effects between proteins *in vivo* (Supplementary Material, Table S3) (40). In this approach, competitive effects between proteins are indicated by a
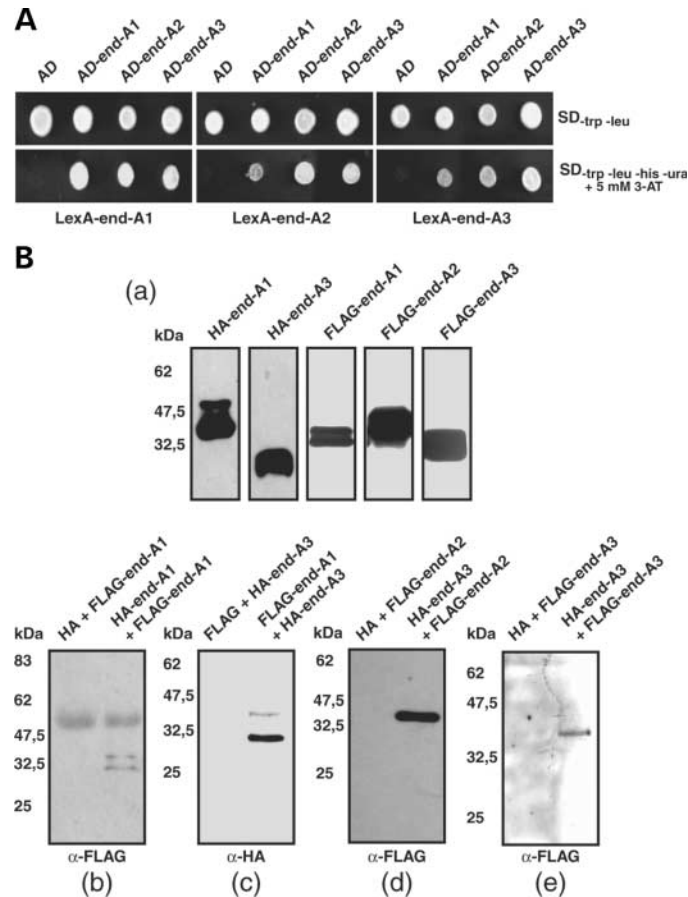
Figure 4. Endophilin-A proteins interact with each other. (**A**) Yeast was co-transformed with the different endophilin bait and prey plasmids in the various combinations as indicated, and transformants were spotted onto selective media for investigating reporter gene activity. Because the LexA-endophilin proteins were slightly autoactivating the reporter genes in the presence of the activation domain alone, 5 mM 3-aminotriazole (3-AT, Sigma) was added to the medium. (**B**) (a) Lysates of COS-1 cells expressing the various HA- or FLAG-tagged versions of the endophilin proteins. (b–e) About 80–120 µg of the different cell extracts were used and mixed in the various combinations as described. After incubation with α-HA or α-FLAG antibodies, co-immunoprecipitation was performed. Precipitates were separated by a 12.5% SDS–polyacrylamide gel and analyzed by immunoblotting using α-HA or α-Flag antibodies.

reduction in the relative activity of the *LacZ* reporter gene. We have generated plasmid p426-HD1(Q25) to overexpress httex1 in the presence of the bait protein LexA–ATX2(Q22)$_{1-396}$ and the prey protein AD-end-A3 in yeast. As controls, we used the empty plasmid p426GPD and the plasmid p426-GFP encoding the green fluorescent protein. Yeast cells expressing the relevant proteins were grown until logarithmic phase, and a liquid β-galactosidase assay was performed to analyze the relative activity of the *LacZ* reporter gene. We discovered that yeast cells co-expressing LexA–ATX2(Q22)$_{1-396}$ and AD-end-A3 show a significant reduction of the *LacZ* reporter gene activity in the presence of overexpressed httex1. In contrast, no reduction of *LacZ* activity was observed in yeast cells expressing the unrelated green fluorescent protein or containing the empty vector (Fig. 5A, left panel). Moreover, a competitive effect of httex1 is also detected in yeast expressing LexA–ATX2(Q79)$_{1-396}$ and AD-end-A3 (Fig. 5A, right panel). A substantial difference in the competitive effects between ATX2(Q22) and ATX2(Q79) was not observed, supporting our earlier observation that the interaction between ATX2 and endophilin-A3 appeared not to be affected by the

length of the polyglutamine stretch (Fig. 1B, right panel). To exclude the possibility that the reduction of *LacZ* reporter gene activity is not due to reduced expression levels of the respective bait and prey proteins, we analyzed their intracellular levels by immunoblotting (Fig. 5B). When compared with the controls, no reduction in expression levels of bait and prey proteins was detected in cells overexpressing httex1. Thus, interplay of huntingtin and ATX2 for binding endophilin-A3 occurs in yeast.

Overexpression of ATX2, endophilin proteins or huntingtin leads to toxic effects in Δ*sac6* yeast

It has been described that endophilin proteins as well as huntingtin play important roles in endocytic vesicle formation or actin filament formation (29,30,38,41–45). Valuable insights into these processes have been obtained for the huntingtin protein using yeast as a model (46,47). To learn more about a potential function of ATX2 within this cellular context, we have screened an assortment of 114 yeast strains deleted for genes involved in these processes for a potential toxic effect
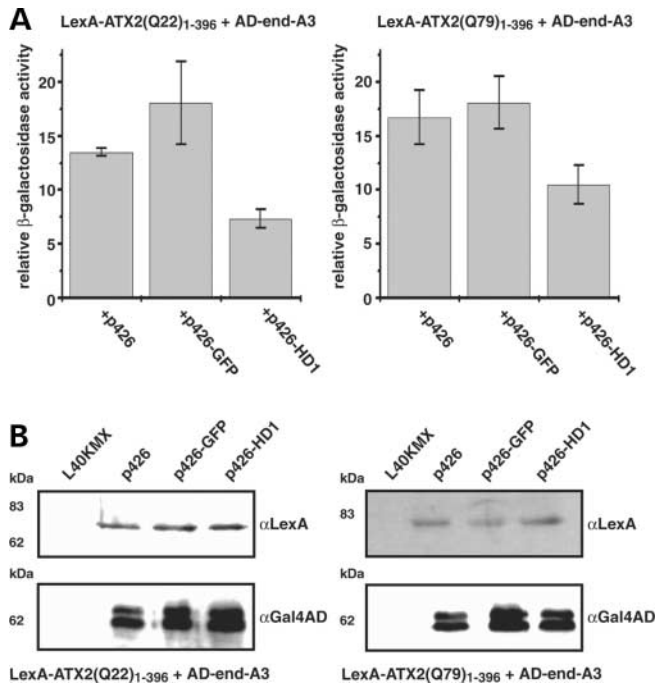
Figure 5. Competitive effects between ATX2 and huntingtin for binding endophilin-A3. (**A**) The relative activity of the *LacZ* reporter gene in the different yeast transformants was measured by a liquid β-galactosidase assay. For the calculation of the standard deviation, four yeast clones of each transformation were used for measurements, and the Nalimov method was applied. (**B**) Yeast lysates were prepared as described and analyzed by 10% SDS−polyacrylamide gels. Proteins were visualized by immunoblotting using α-LexA or α-Gal4AD antibodies.

of normal as well as mutant ATX2 (Supplementary Material, Table S4). Selected deletion strains were transformed with plasmids encoding full-length ATX2 with 22 or 79 consecutive glutamines, placed under the control of a galactose-inducible promoter. As control, the empty vector p423GALL was used. Subsequently, transformants were grown on plates containing raffinose as carbon source and afterwards, transferred to the respective medium plates containing galactose for induction of ATX2. Growth of the various yeast strains on galactose plates was analyzed, and strains that showed reduced growth when compared with the empty plasmid have been selected for further analysis. To validate the observed growth defect, the respective strains were transformed with the corresponding plasmids yet again. Next, transformants were grown overnight in raffinose-containing medium and spotted in 5-fold serial dilutions onto galactose plates for induction of ATX2 proteins. From the 114 yeast deletion strains investigated, the most prominent toxic effect of ATX2 expression was observed in yeast lacking the *SAC6* gene, which encodes the yeast protein fimbrin (Fig. 6A, left panel). Both, expression of ATX2 with 22 or 79 consecutive glutamines led to reduced growth of Δ*sac6* yeast on galactose plates demonstrating that the observed toxic effects are independent of the length of the glutamine stretch in ATX2. This toxic effect was neither observed on glucose plates (no expression of ATX2) nor led ATX2 expression to reduced growth in the wild-type yeast strain BY4741.

To verify that the observations made are specific due to *SAC6* gene deletion and not an artificial phenomenon, we expressed the two human functional orthologs of yeast fimbrin, termed L- and T-plastin, in the presence of ATX2 in the Δ*sac6* yeast strain; both proteins have been shown to complement the defects in cytoskeletal organization and cell morphology of Δ*sac6* yeast cells (48). We have amplified the full coding sequence of L- and T-plastin from a human fetal brain cDNA library (Clontech) and subcloned the respective DNA fragments into the low-copy plasmid p416GPD (49). As shown in Figure 6A (right panel), constitutive expression of both human plastin proteins diminished the toxic effect caused by expression of ATX2 with 22 or 79 glutamines confirming that the observed toxicity of ATX2 is indeed caused by loss of the yeast fimbrin protein.

In addition, we have included the endophilin proteins and huntingtin in our analysis. Therefore, Δ*sac6* yeast cells have been transformed with galactose-inducible plasmids encoding endophilin-A1, endophilin-A3 or httex1 with 25 consecutive glutamines. We discovered that expression of both endophilin proteins led to almost lethal effects in Δ*sac6* yeast (Fig. 6B, left panel), whereas expression of httex1 caused a milder, but significant growth defect (Fig. 6C, left panel). Similarly, co-expression of human L- or T-plastin lessened the observed toxic effects caused by expression of endophilin-A1, endophilin-A3 or httex1 (Fig. 6B and C, right panels). To exclude that the observed effects in this strain background are not simply caused due to a protein's overexpression, we included the unrelated green fluorescent protein as control; no reduced growth of the respective yeast clones were observed (data not shown). Thus, endophilin proteins, huntingtin and ATX2 appear to be implicated in related cellular pathways.

ATX2 forms complexes with L- and T-plastin in mammalian cells and its overexpression leads to cytoplasmic accumulation of human T-plastin

To substantiate the relevance of the interplay between ATX2, endophilins and huntingtin in a related pathway, we explored if the genetic relationship may point to a direct physical interaction or cellular complex formation. In the first step, we investigated whether a physical interaction between ATX2, the endophilin proteins or huntingtin and L- or T-plastin occurs in the yeast-two-hybrid system. Therefore, strain L40ccua was transformed with the various bait and prey plasmids encoding different ATX2 regions, endophilin-A1, endophilin-A3 or httex1 as well as different regions of L- and T-plastin. However, a direct interaction between ATX2, endophilin proteins or httex1 and L- or T-plastin was not observed under the chosen experimental yeast-two-hybrid conditions (data not shown). Nonetheless, we performed co-immunoprecipitation experiments to investigate whether an association of these proteins occurs in mammals. Using mouse brain lysate, ATX2 was precipitated applying antibodies directed against L- and T-plastin indicating complex formation of ATX2 with both plastin isoforms (Fig. 7A). Additionally, we were able to confirm this result by performing co-immunoprecipitation using COS-1 cells co-expressing recombinant full-length HA-tagged ATX2 and FLAG-tagged L- or T-plastin, using an antibody directed against the FLAG tag (data not shown).
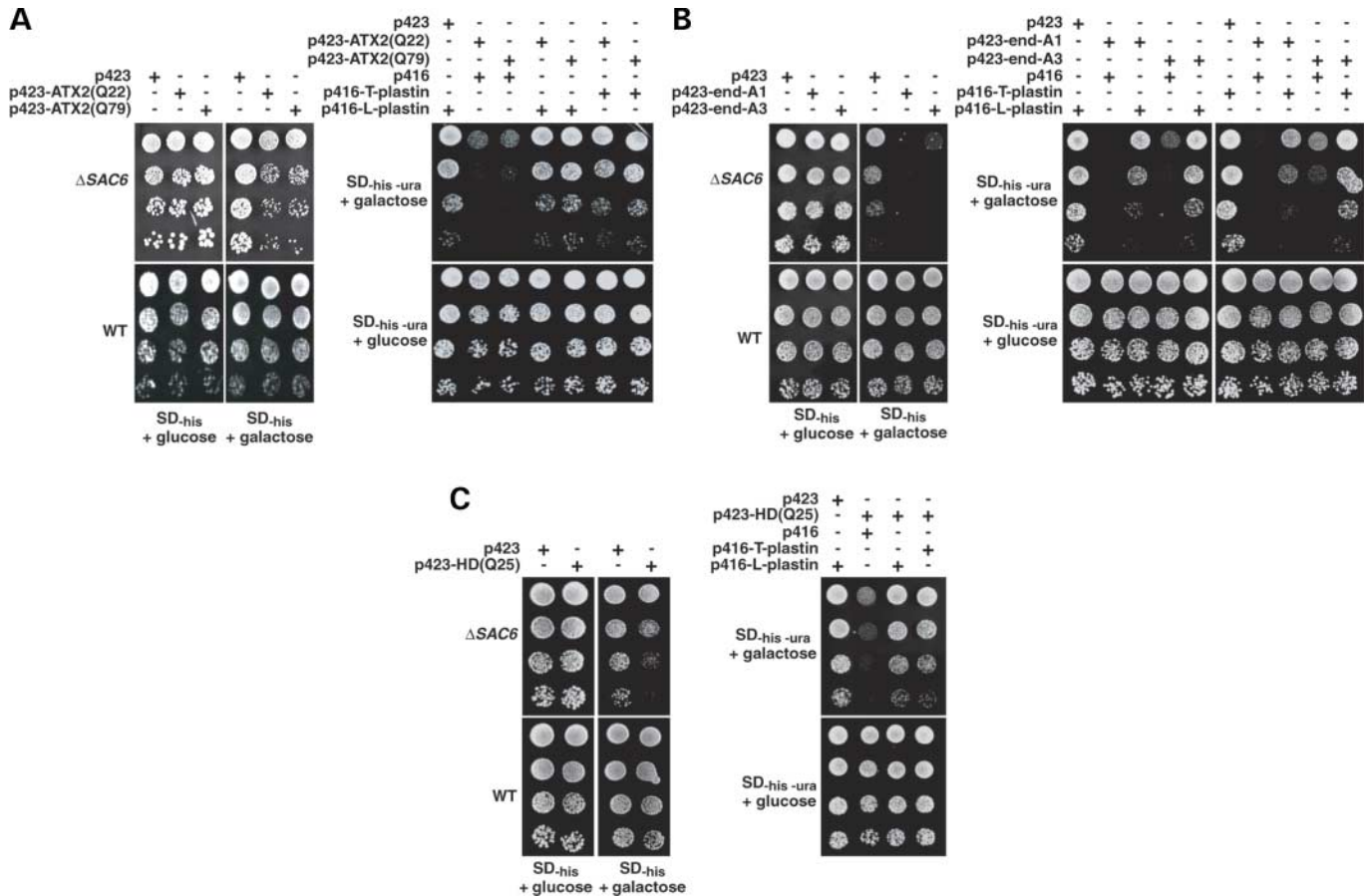
Figure 6. Overexpression of ATX2, endophilin proteins, and httex1 is toxic in Δ*sac6* yeast cells. (**A**) Left panel: wild-type strain BY4741 and the isogenic Δ*sac6* strain were transformed with plasmids p423 as control, p423-ATX2(Q22) or p423-ATX2(Q79). The resultant transformants were spotted as 5-fold serial dilutions onto the respective medium plates containing glucose or galactose for induction of ATX2 expression as carbon source. Right panel: Δ*sac6* yeast was co-transformed with the different p423 plasmids in combination with p416 (control), p416-L-plastin or p416-T-plastin. Single yeast clones from each transformation were isolated and grown in selective media containing 2% raffinose. Afterwards, equal cell numbers of each yeast culture was spotted as 5-fold serial dilution onto the selective medium supplemented with 2% glucose or 2% galactose. (**B**) Left panel: wild-type and Δ*sac6* yeast cells were transformed with plasmids p423, p423-end-A1 or p423-end-A3. Transformants were isolated and spotted onto the media plates as described in (A). Right panel: Δ*sac6* yeast was co-transformed with p423-based plasmids encoding endophilin-A1 or endophilin-3 in combination with p416, p416-L-plastin or p416-T-plastin. (**C**) Left panel: wild-type and Δ*sac6* yeast cells were transformed with plasmids p423 or p423-HD(Q25) and analyzed as described in (A). Right panel: Δ*sac6* yeast was co-transformed with p423-based plasmids encoding httex1 with 25 glutamines in combination with p416, p416-L-plastin or p416-T-plastin. As controls, yeast containing the empty vectors p423 and p416-L-plastin or p416-T-plastin was included. Growth of the various yeast strains on the different selective media was analyzed after incubation of plates for 3–5 days at 30°C.

Next, we have performed immuofluorescence microscopy for ATX2 and the two plastin isoforms in mammalian cell lines. HEK293T or SH-SY5Y cells were fixed and stained with antibodies directed against ATX2 and L-plastin or ATX2 and T-plastin (Fig. 7B). We discovered that ATX2 and the plastin isoforms are located in the cytoplasm of mammalian cells, and co-localize in the perinuclear area. This supports that cytoplasmic complexes comprising ATX2 and plastin proteins are formed in mammalian cells.

Intriguingly, we observed that overexpression of ATX2 with a stretch of 22 or 79 glutamines causes a strong cytoplasmic accumulation of endogenous T-plastin in mammalian cell lines as analyzed by confocal immunoflourescence microscopy (Fig. 8A(a and c)). However, no change of the endogenous L-plastin level was detected in the respective cell lines

overexpressing ATX2 (Fig. 8A(b and d)). Increased T-plastin levels have been also observed in COS-1 cells overexpressing ATX2. Here, a quantitative analysis has been performed and showed indeed an increase of T-plastin immunoreactivity in ATX2-transfected cells when compared with that in non-transfected cells (Fig. 8B(a and b)); no increase in L-plastin immunoreactivity was detected (Fig. 8B(c and d)). Finally, we investigated whether overexpression of either endophilin proteins or httex1 had an effect on endogenous L- and T-plastin immuno-reactivity. However, we observed no alterations of endogenous L- and T-plastin levels in mammalian cells overexpressing these proteins (data not shown), indicating that the effect of ATX2 overexpression on the cellular T-plastin concentration is specific. Thus, these results confirm yet again a cellular interplay between ATX2 and plastin proteins.
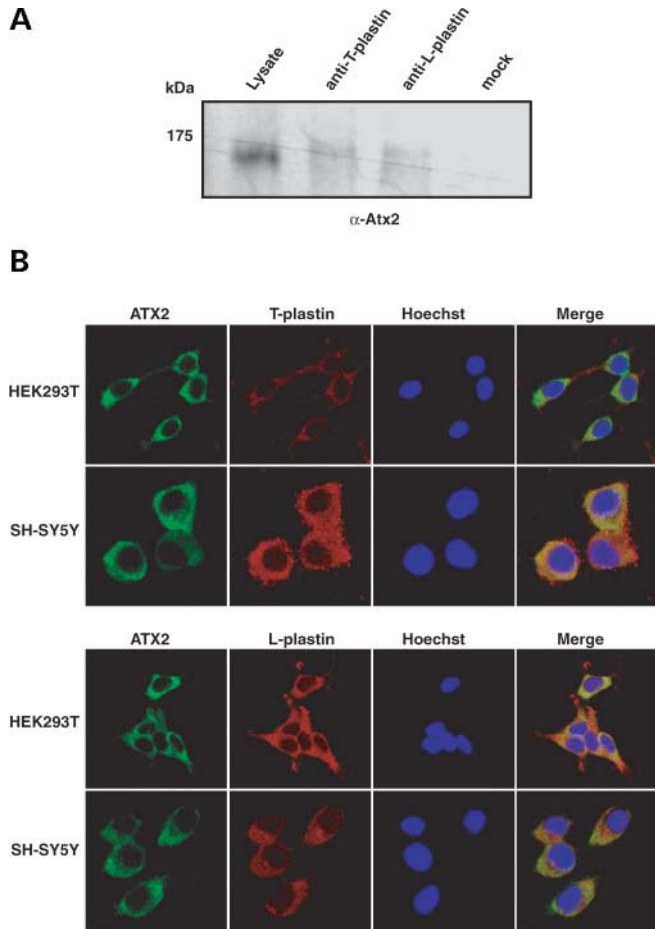
Figure 7. L-plastin and T-plastin form complexes with ATX2 (**A**) Mouse brain was lysed and incubated with antibodies directed against α-L-plastin or α-T-plastin. Precipitates were analyzed by SDS–PAGE and immunoblotted using α-ATX2 antibody. (**B**) Endogenous levels of ATX2 and L-plastin or T-plastin were visualized using α-ATX2, α-L-plastin or α-T-plastin as indicated in HEK293T and SH-SY5Y cells. Nuclei were stained with Hoechst.

DISCUSSION

In this study, we have identified and established a link between ATX2 and two members of the endophilin family, endophilin-A1 and endophilin-A3. Members of the endophilin-A family are evolutionarily conserved, paralogous proteins comprising two major domains, an N-terminal BAR-domain and a C-terminal Src homology-3 (SH3) domain, the latter of which represents one of the most common domains in eukaryotic organisms. The cellular function of the BAR domain still needs to be clarified, but it has been recently proposed that the BAR domain generally functions as dimerization motif and may induce membrane curvature or associate with small GTPases (50). In contrast, the SH3 domain is usually responsible for driving protein–protein interactions through its binding to proline-rich peptides (33). An involvement of the endophilin-A proteins in various cellular processes has been suggested partly because of their different expression pattern as well as their interplay with different cellular factors. Endophilin-A2 is ubiquitously expressed, whereas endophilin-A1 is preferentially expressed

in the brain, and endophilin-A3 is predominantly detected in brain and testis (28,38,51–53). Owing to the association of endophilin-A proteins with amphiphysin I and II (42), dynamin or synaptojanin I (52,54), a role in clathrin-mediated endocytosis has been proposed, hence, their exact role remains to be studied in detail. Functionality of endophilin proteins in late endocytosis steps has been demonstrated (51,55). Endophilin-A1 is a multifunctional protein found in association with signaling molecules and its overexpression leads to JNK pathway activation, which points to an important role in cell cycle regulation (45,56). Localization of endophilin-A2 to specific actin scaffolds has been observed (57). Furthermore, endophilin-A3 does co-localize to some extent with actin filaments; however, it is associated to a greater extent with microtubules in a dynamic manner, suggesting a function in transport processes (41). Therefore, it has been proposed that endophilin-A proteins may represent adaptor proteins that coordinate and link other cellular events such as actin function and signaling cascades to endocytotic pathways (45).

Remarkably, endophilin-A3 has been reported to interact with the polyglutamine protein huntingtin (31). Interaction between both proteins depends on the SH3 domain and the proline-rich region following the polyglutamine region in exon 1 of huntingtin (31,58). In our study, we have characterized the interaction between ATX2 and both endophilin-A1 and endophilin-A3. We have demonstrated that the interaction of the proteins depends on the SH3 domain in endophilin-A1 and endophilin-A3 and the two SH3 binding motifs, SBM1 and SBM2, in ATX2. Endophilin-A3 binds to both binding motifs, whereas endophilin-A1 associates only with the C-terminal one, SBM2. However, we have demonstrated that endophilin-A3 interacts with endophilin-A1 and endophilin-A2 in yeast and forms homologous and heterologous complexes in mammalian cells.

Furthermore, we have shown that the interaction between ATX2 and endophilin-A3 can be influenced by simultanous co-expression of huntingtin in yeast, suggesting an important interplay between these proteins in the cellular environment. Along this line, we have presented additional data, suggesting functionality of ATX2, endophilin proteins and huntingtin in plastin-associated pathways. We have discovered that the expression of ATX2, both endophilin-A proteins and huntingtin leads to toxicity in yeast cells lacking the *SAC6* gene. The respective gene product, termed fimbrin, co-localizes with actin patches and actin cables and associates with actin structures that are implicated in the development and maintenance of cell polarity (59,60). Moreover, fimbrin functions in actin bundling *in vitro* and stabilizes actin filaments *in vivo* (59,61). Accordingly, yeast lacking fimbrin displays a decrease in actin filament assembly and is defective in endocytotic processes (61,62). Yeast fimbrin has two functional human homologs, termed L- and T-plastin, which show a significant sequence identity of 40% to yeast fimbrin, and can suppress the phenotype of Δ*sac6* yeast (48). Here, we have demonstrated that the toxic effects of ATX2, endophilins and huntingtin observed in yeast are caused through a loss of fimbrin, because the simultaneous expression of human L- or T-plastin lessens the toxicity in either case.

Plastins belong to a family of highly conserved actin binding and bundling proteins and have been implicated in
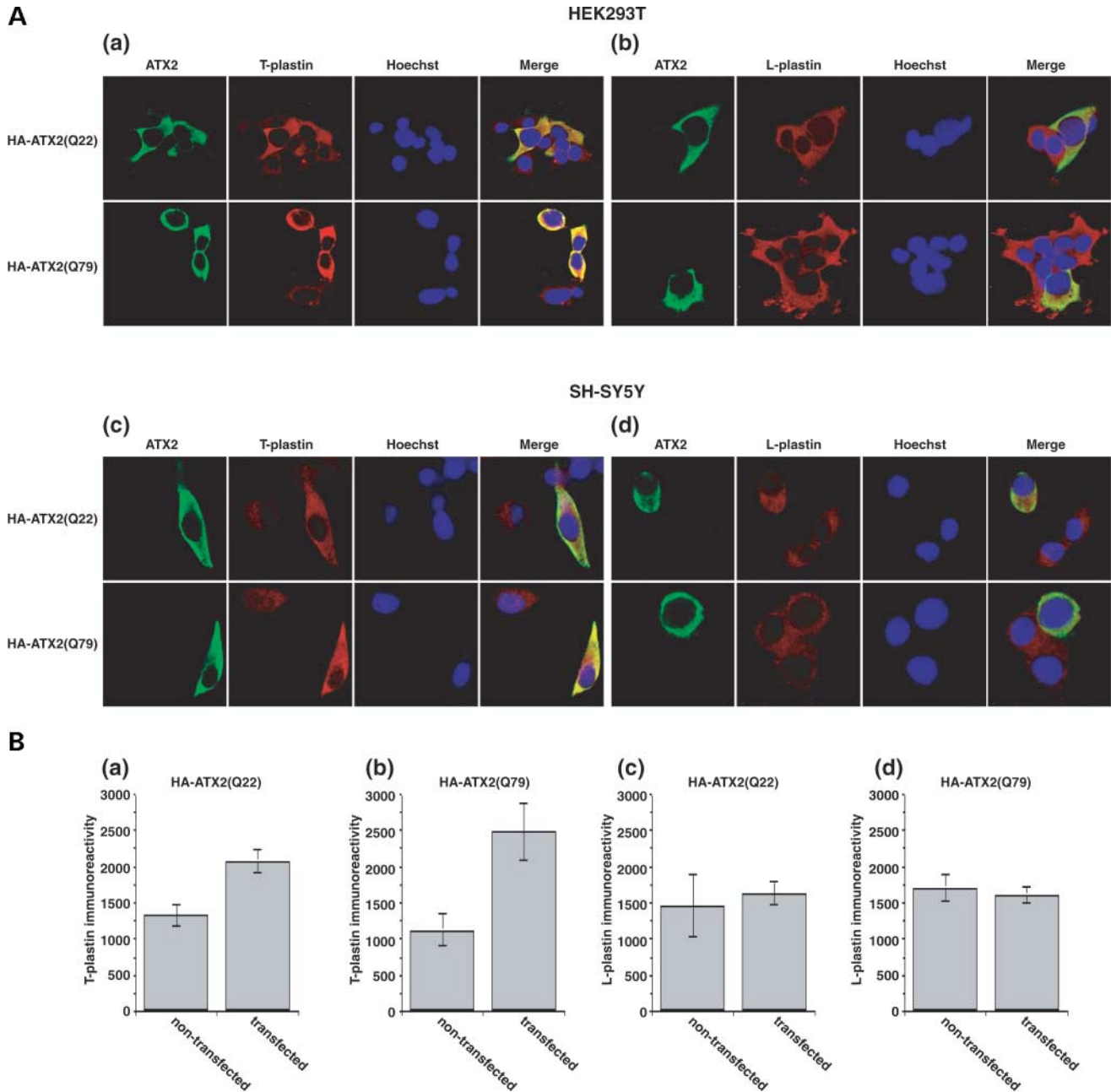
Figure 8. T-plastin immunoreactivity is increased in mammalian cells overexpressing ATX2. (**A**) HEK293T cells (a and b) as well as SH-SY5Y cells (c and d) have been transiently transfected with plasmids pTL-HA-ATX2(Q22) or pTL-HA-ATX2(Q79), and cells were analyzed by immunofluorescence microscopy. For staining overexpressed HA-tagged full-length ATX2, cells were incubated with an α-HA antibody and with α-T-plastin or α-L-plastin antibodies to visualize endogenous levels of T-plastin or L-plastin. Nuclei were stained with Hoechst. (**B**) Quantitative analysis of T- and L-plastin immunoreactivity in COS-1 cells using Axiovision software (Zeiss). The values represent the mean flourescent intensity per square micrometers.

various cellular processes such as regulation of cell morphology, bacterial invasion and tumor progression (48,63–67). They are structurally composed of two actin-binding domains, four calponin-homology and two EF-hand calcium-binding domains (68) and are known to stabilize actin filament structures by their actin-bundling activity. This activity seems to be modulated differently by calcium concentration (69,70). The most characterized isoforms L- and T-plastin are differentially expressed and both play roles in actin filament organization in a cell type specific manner (67,70). Both proteins exhibit a different nucleocytoplasmic trafficking behavior (65). Here, we have discovered an interaction of ATX2 with both L- and T-plastin in mouse brain, linking ATX2 to pathways that play a role in actin filament formation and organization. This finding is intriguing in the light of the *Drosophila melanogaster* ATX2 homolog (DATX2) that seems to be involved in regulating actin filament formation (71). Both reduced activity and overexpression of wild-type

DATX2 lead to severe phenotypes in flies, presumably resulting from alterations in actin filament formation and organization. Because neither changes in intracellular concentration of actin nor an interaction of DATX2 with actin was observed, it has been suggested that DATX2 acts on translation stability or localization of transcripts encoding mediators of actin polymerization (71). Noticeably, we have discovered that overexpression of ATX2 in mammalian cells leads to an increased immunoreactivity of T-plastin, whereas L-plastin levels were not altered; in cells overexpressing the endophilin proteins or httex1, no increase in immunoreactivity of T-plastin was detected. As reported previously, T-plastin decreases the disassembly rate and inhibits cofilin-mediated depolymerization of actin filaments *in vitro* and is involved in controlling actin turnover as well as the length of actin filaments in structures *in vivo* (66). Therefore, it is very likely that higher concentrations of T-plastin prevent actin turnover by abnormal cross-link formation and filament stabilization, causing alterations in actin dynamics. Nevertheless, the effect of a high T-plastin level could be indirect because interference with other actin-binding proteins or other essential cellular proteins could occur. Interestingly, abnormal expression of T-plastin has been observed in many carcinomas (72–74). In addition, increased levels of T-plastin have been observed in CHO cells after DNA damage (75) and correlated with the differentiating potential of cytotrophoblast and syncytiotrophoblast cells during placental development (76). Along these lines, overexpression of fimbrin in the yeast *Saccharomyces cerevisiae* leads to a severe phenotype that might be caused by a less dynamic actin cytoskeleton due to hyperstabilization (77). In fission yeast, the fimbrin-like protein Fim1 that is a component of both F-actin patches and F-actin rings seems to play a role in the stabilization of F-actin patches and could function together with other proteins in cytokinesis (78).

The proteins causing polyglutamine disorders show no structural similarities and evolutionary relationships except the glutamine stretch. However, a functional role of polyglutamine proteins in a common or related pathway has often been discussed and searched in the past (12,79,80). Here, we have provided evidence that ATX2 and huntingtin are functionally connected through an interaction with endophilin-A complexes. Interestingly, Ringstad *et al.* (38) have initially described that homodimer formation of endophilin-A1 as well as heterodimer formation of endophilin-A1 and endophilin-A2 occurs. In this work, we have demonstrated that endophilin-A3 interacts with the other two members as shown by yeast-two-hybrid studies as well as by mammalian cell culture experiments, supportive of a complex cellular interplay of endophilin proteins.

Clearly, additional work is required to understand the exact functional role of ATX2 and huntingtin in the cellular pathways discovered here. First, it would be interesting to analyze whether and how other polyglutamine proteins are involved in endophilin-associated pathways. For instance, ataxin-7 interacts through its proline-rich regions after the polyglutamine stretch with SH3 domains of a Cbl-associated protein (CAP, pontin, SORBS1, SH3P12) (81). This SH3 domain protein may also bind huntingtin (82) and belongs to a novel family of adaptors including ArgBP2 and vinexins

that regulate cytoskeletal organization and signal transduction as well (83). Therefore, it might also be worthwhile to test ataxin-7 for association with endophilins. Moreover, it would be valuable to explore members of the endophilin-B family for a functional interplay with the polyglutamine proteins, because endophilin-B1, which itself binds amphiphysins, dynamin and synaptojanin like the endophilin-A proteins, interacts with huntingtin (84).

Secondly, we demonstrated that ATX2 associates with both plastin forms. Interestingly, proteomics-based results show that T-plastin and PABP as well as their corresponding yeast homologs fimbrin and Pab1 have been observed to be contained together in large protein complexes of 216 subunits and 39 subunits mainly consisting of proteins involved in RNA processing (85,86). This observation is quite remarkable in the light that ATX2 directly interacts with the cytoplasmic PABP (25). Therefore, future investigations should focus on the functional relationship of T-plastin and PABP with regard to RNA metabolism.

Finally, it is noteworthy that alterations of intracellular ATX2 as well as plastin levels have been observed in various disorders. As mentioned earlier, plastin levels are modified in certain carcinomas, hence, the impact on cellular level remains to be elucidated. Increased cellular concentration of ATX2 has been implicated in the progression of neuroblastomas of children (87). Most strikingly, enhanced levels of ATX2 have been observed in Purkinje cells of humans with age, as well as in Purkinje cells of SCA2 patients (18,21). In the future, elucidating the consequences of increased expression levels of ATX2 for the cellular network will provide valuable informations about the pathways that might contribute to SCA2 pathogenesis and, additionally, to cancer. Morphological changes of Purkinje cells that could be based on disturbances in actin metabolism have been observed in the mouse SCA2 disease model (19). Our findings might also help to discover molecular mechanisms contributing to Huntington's disease, because both polyglutamine proteins, ATX2 and huntingtin, function in related pathways.

MATERIALS AND METHODS

Plasmids

Plasmid constructions are described in Supplementary Material, Tables S1 and S2.

Antibodies

The following antibodies were used in our immunoblot analyses in the indicated dilutions: mouse α-FLAG (1:5000, Sigma), rabbit α-FLAG (1:5000, Sigma), mouse α-HA (1:5000, Roche), rabbit α-cMYC (1:4000, Sigma), mouse α-ATX2 (1:400, BD Biosciences), polyclonal rabbit serum directed against LexA (1:5000) (40), rabbit α-Gal4AD (1:1000, Sigma) or rabbit α-GST (1:5000, Zymed).

Yeast strains, cultivation and lysate preparation

The yeast strains used in this study are listed in Supplementary Material, Tables S3 and S4. For cultivation, yeast strains

L40ccua, L40ccα and BY4741 were grown in rich medium (YPD) supplemented with 2 % glucose. Strain L40KMX and the respective yeast deletion strains were incubated in YPD medium supplemented with 200 µg/ml G418 sulfate (Gibco) and 2% glucose. Transformation of yeast strains was performed by the lithium acetate method (88). For preparation of yeast lysates, single yeast clones were incubated overnight at 30°C, subsequently transferred into fresh media and grown until logarithmic phase. After centrifugation of the same number of yeast cells, the cell pellets were resuspended in ice-cold ethanol. About 200 µl glass beads (425–600 µm, Sigma) were added, samples were intensively shaken for 5 min at 4°C and the supernatants were collected. This procedure was repeated for three times. Proteins were precipitated for 60 min at −20°C. After centrifugation, precipitates were resuspended in phosphate-buffered saline (PBS) containing 1 mM phenylmethansulfonylfluorid (Sigma). The total protein concentration was determined using a Bradford assay (BioRad). Then, 50 µg of each sample was heated in Laemmli buffer for 5 min at 95°C and separated by SDS–PAGE. Proteins were transferred to nitrocellulose membranes (Schleicher and Schuell) using a PerfectBlue semidry electroblotter (PeqLAB). Subsequently, membranes were blocked in 5% milk solution for 1 h at room temperature or overnight at 4°C. Afterwards, membranes were incubated with the primary antibodies α-LexA or α-Gal4AD for 1 h, washed in PBS and incubated with peroxidase-conjugated secondary antibodies (1:5000, Sigma). To visualize the proteins, the membranes were incubated with 'western-lightning' solution (Perkin Elmer) and exposed to a BioMax XAR film (Kodak).

Yeast-two-hybrid analysis

Strain L40ccua was co-transformed with plasmids pGAD and pBTM-ATX2-NT(Q22), pGAD and pBTM-ATX2-FB, pGAD and pBTM-ATX2-FC or pGAD and pBTM-ATX2-FD to exclude that LexA–ATX2 proteins can activate the three reporter genes *URA3, HIS3* and *LacZ per se* in yeast. Afterwards, the respective transformants were tested for autoactivation of the reporter genes by transferring selected yeast clones on SD media lacking tryptophan, leucine, histidine and uracil or on nylon membranes [Micron Separation Inc., (MSI)] for analyzing *LacZ* activity. Plates were incubated for 48–72 h at 30°C, and growth of yeast on selective media was analyzed. For testing the *LacZ* reporter gene activity, yeast cells were lysed in liquid nitrogen. Hereafter, membranes were incubated on Whatman paper saturated with X-Gal buffer [phosphate buffer (pH 7.0), 0.15% X-Gal, 10 mM dithiothreitol (DTT)] for up to 4–6 h at 37°C, and yeast clones were analyzed for color shift. In addition, we would like to point out that our directed yeast-two-hybrid studies were performed in the same way.

For the yeast-two-hybrid analyses, we have performed a mating approach applying a yeast-two-hybrid-array consisting of 5760 prey clones based on yeast strain L40ccα (Stelzl *et al.*, *Cell*, in press, doi:10.1016/S0092867405008664). The relevant bait yeast strains have been generated by transforming plasmid pBTM-ATX2-NT(Q22), pBTM-ATX2-FC or pBTM-ATX2-FD into yeast strain L40ccua. Each of the bait strains was mated with the yeast-two-hybrid-array on YPD

media. After mating, yeast was spotted onto media lacking tryptophan and leucine for selection of diploid yeast clones. Subsequently, yeast clones were tested for the activity of the reporter genes *HIS3* and *LacZ* by spotting yeast clones onto the respective SD media lacking tryptophan, leucine and histidine. For testing *LacZ* activity, yeast clones were spotted onto nylon membranes (MSI). After incubating the plates for 2–3 days at 30°C, growth of yeast on the respective SD media was analyzed, and activity of the *LacZ* reporter gene was determined as described earlier. Yeast clones that showed activation of both reporter genes indicative of a potential protein–protein interaction were selected. To verify the observed protein–protein interaction, mating of the corresponding bait and prey pair was performed yet again. Additionally, strain L40ccua was co-transformed with plasmids encoding the respective lexA–ATX2 protein as well as the relevant prey protein to verify the observed interaction in an independent experiment as described earlier. For measuring the relative activity of the *LacZ* reporter gene, a liquid β-galactosidase assay was carried out as described earlier (40).

Cell culture

COS-1, HEK 293, HEK293T and SH-SY5Y cells were grown in a humidified 5% CO₂ atmosphere at 37°C in Dulbecco's modified Eagle medium (DMEM, Gibco) supplemented with 5% heat inactivated fetal bovine serum (Biochrom), 50 U/ml penicillin (Biochrom) and 50 µg/ml streptomycin (Biochrom). For differentiation of SH-SY5Y cells, DMEM was supplemented with 20 ng/ml nerve growth factor (Invitrogen). Transfection was performed using Polyfect (Qiagen) as recommended by the manufacturer.

Co-immunoprecipitation

COS-1 cells were transfected with the respective plasmids and incubated for 48 h at 37°C to allow expression of recombinant proteins. Afterwards, cells were washed in PBS and incubated for 30 min on ice in lysis buffer (50 mM Tris–HCl, 100 mM NaCl, 5 mM MgCl₂, 0.5% NP-40, 1 mM EDTA, pH 8.8, 25 U/ml benzonase (Merck) and 2.5% protease inhibitors ('complete' tablets, Roche). Protein concentration of lysates was determined by a Bradford assay (Bio-Rad). About 100–130 µg of each cell lysate was incubated with 1 µl of mouse α-HA antibody (Roche), 1 µl of rabbit α-FLAG antibody (Sigma) or 1 µl of rabbit α-cMYC antibody (Sigma) for 2–3 h at 4°C on a rotating wheel. Afterwards, 15 µl IgG-conjugated Dynabeads M-280 (Dynal) were added to each lysate, and samples were incubated for 3 h at 4°C on a rotating wheel. Dynabeads were pulled down magnetically, and beads were washed three times in PBS containing 3% bovine serum albumin (BSA) (Sigma) and finally in PBS. Bound protein was eluted from Dynabeads by heating samples in Laemmli buffer for 5 min at 95°C and subsequently analyzed by immunoblotting as described.

Mouse brain extract from a 6-month-old female NMRI mouse was prepared from one whole brain, which was homogenized in 2 ml extraction buffer [50 mM HEPES–KOH (pH 7), 150 mM NaCl, 10% glycerol, 1% NP-40, 1 mM EGTA (pH 7), 20 mM NaF, 1 mM DTT, 1.5 mM MgCl₂, one tablet

of EDTA-free complete protease inhibitor (Roche) per 10 ml extraction buffer] on ice. After centrifugation, the supernatant fraction was collected. One milligram of brain extract was incubated with 1.5 μl α-L-plastin or α-T-plastin and incubated for 5 h on a rotating wheel at 4°C. Afterwards, 30 μl of M-280 Dynabeads (Dynal) were added and incubation was carried out overnight at 4°C. The following steps were performed as described earlier.

In silico approach for predicting binding motifs

To determine the positions of binding sites for SH3 domain proteins in ATX2 and ATX2L, we applied the bioinformatics methods ELM (89), iSPOT (90) and Scansite (91), which are available online. UniProt accession numbers of sequences used are Q99700 and O70305 for human and mouse ATX2, Q8WWM7 and Q7TQH0 for human and mouse ATX2L and Q99962/Q99961/Q99963 for endophilin-A1/A2/A3.

Cross-link assay

Expression plasmids pGEX-SBM1 as well as pGEX-SBM2 encoding the predicted ATX2-endophilin binding motifs fused to the GST protein were created as described in Plasmids, Supplementary Material, and transformed in *Escherichia coli* strain SCS1. Expression of pure GST protein and GST fusion proteins was induced by adding 1 mM isopropyl-beta-D-thiogalactopyranoside (IPTG, Sigma) to the relevant *E. coli* cultures. Cultures were incubated overnight at 15°C, and pure GST and GST fusion proteins were purified using glutathione–Sepharose (BD Bioscience). One microgram of each purified GST protein was incubated with 100 μg total cell lysate that has been derived either from COS-1 cells that have been transiently transfected with expression plasmids pTL-Flag-end-A1 or from pTL-Flag-end-A3. As mock control, cell lysate without additional GST-protein was used. After incubating the samples on a rotating wheel for 1 h at 4°C, samples were cross-linked using dithio-bis-[succinimidylpropionate] (DSP, Pierce) as recommended by the manufacturer. Subsequently, 1 μl of mouse α-FLAG IgG was added, and samples were incubated for 30 min at 4°C. Afterwards, 15 μl anti mouse-IgG antibodies coupled to Dynabeads were added, and the samples were incubated for 2 h at 4°C on a rotating wheel. Dynabeads were washed three times in PBS containing 3% BSA and once in PBS. Bound protein was eluted from Dynabeads by heating samples in Laemmli buffer for 5 min at 95°C and subsequently analyzed by immunoblotting as described.

Yeast deletion strain screen

One-hundred and fourteen yeast strains deleted for genes involved in endocytosis, vesicle transport and actin filament formation were selected from the yeast deletion strain library by database analysis using the *S. cerevisiae* genome database (92) (selected strains are listed in Supplementary Material, Table S4) and transformed with plasmids p423GALL, p423-ATX2(Q22) or p423-ATX2(Q79) for inducible expression of full-length ATX2 protein containing a stretch of 22 or 79 glutamines. Transformants were plated on minimal media lacking the amino acid histidine supplemented with 2% glucose, and plates were incubated for 3 days at 30°C. Afterwards, single yeast colonies were selected and grown on selective media supplemented with 2% raffinose as carbon source. Freshly grown yeast clones were transferred onto media containing galactose as carbon source to induce the expression of ATX2 and incubated for 3–5 days at 30°C. Candidate strains that showed reduced growth in the presence of ATX2 protein were selected. To verify the observed toxicity of ATX2 in the respective yeast background, the candidate strains were transformed again with the corresponding yeast expression plasmids. Subsequently, single yeast colonies were incubated in liquid media supplemented with 2% raffinose until an OD$_{600}$ of 0.7–1.0. Equal cell numbers of each culture was spotted as a 5-fold dilution series onto the respective selctive medium supplemented with 2% glucose or with 2% galactose as carbon source, and plates were incubated for 3–5 days at 30°C.

Microscopic analysis

The respective mammalian cell lines described earlier have been transfected and incubated for 48 h to allow expression of proteins. For endogenous localization studies, cells have been grown on glass slides for 24 h before cells were fixed with 4% paraformaldehyde for 15 min at room temperature. Then, cells were permeabilized with PBS/0.1% Triton X-100 and treated with PBS/3% BSA for 30 min. For double staining, cells were incubated with primary antibodies directed against ATX2 (1:200, BD Biosciences) and endophilin-A1 (1:100, Zytomed) or ATX2 and endophilin-A3 (1:100) (31) for 1 h at room temperature. For visualization of HA-tagged ATX2 proteins, cells were treated with an antibody directed against the HA-tag (1:400, Roche). The isoforms, L- and T-plastin, were stained with the polyclonal antibodies, α-L-plastin or α-T-plastin using a dilution of 1:200 (93). Subsequently, cells were washed in PBS/0.1% Triton X-100 and incubated with the corresponding secondary antibodies, FITC-conjugated α-mouse IgG (1:400, Dianova) or Cy3-conjugated α-rabbit IgG (1:400, Dianova). Finally, cells were rinsed with PBS/0.1% Triton X-100, and nuclei were stained with Hoechst (bisBenzimide, Sigma). The glass slides were mounted with an antifade medium [1 mg/ml p-phenylendiamine (Sigma), 90% glycerol in PBS], and microscopic pictures were taken with an LSM510 fluorescense microscope (Zeiss).

For the quantification of L- and T-plastin immunoreactivity, COS-1 cells have been transiently transfected with plasmids encoding full-length HA-tagged ATX2 with 22 or 79 consecutive glutamines. Afterwards, cells were fixed and stained as described earlier. Then, at least 10 cytoplasmic regions from randomly chosen ATX2-transfected and non-transfected cells were selected and analyzed using the Axiovision software (Zeiss) for the intenstity of the Cy3 immunoreactivity.

SUPPLEMENTARY MATERIAL

Supplementary Material is available at HMG Online.

REFERENCES

1. Schols, L., Bauer, P., Schmidt, T., Schulte, T. and Riess, O. (2004) Autosomal dominant cerebellar ataxias: clinical features, genetics, and pathogenesis. *Lancet Neurol.*, **3**, 291–304.
2. Moseley, M.L., Benzow, K.A., Schut, L.J., Bird, T.D., Gomez, C.M., Barkhaus, P.E., Blindauer, K.A., Labuda, M., Pandolfo, M., Koob, M.D. *et al.* (1998) Incidence of dominant spinocerebellar and Friedreich triplet repeats among 361 ataxia families. *Neurology*, **51**, 1666–1671.
3. Giunti, P., Sabbadini, G., Sweeney, M.G., Davis, M.B., Veneziano, L., Mantuano, E., Federico, A., Plasmati, R., Frontali, M. and Wood, N.W. (1998) The role of the *SCA2* trinucleotide repeat expansion in 89 autosomal dominant cerebellar ataxia families. Frequency, clinical and genetic correlates. *Brain*, **121** (Pt 3), 459–467.
4. Brusco, A., Gellera, C., Cagnoli, C., Saluto, A., Castucci, A., Michielotto, C., Fetoni, V., Mariotti, C., Migone, N., Di Donato, S. *et al.* (2004) Molecular genetics of hereditary spinocerebellar ataxia: mutation analysis of spinocerebellar ataxia genes and CAG/CTG repeat expansion detection in 225 Italian families. *Arch. Neurol.*, **61**, 727–733.
5. Pulst, S.M., Nechiporuk, A., Nechiporuk, T., Gispert, S., Chen, X.N., Lopes-Cendes, I., Pearlman, S., Starkman, S., Orozco-Diaz, G., Lunkes, A. *et al.* (1996) Moderate expansion of a normally biallelic trinucleotide repeat in spinocerebellar ataxia type 2. *Nat. Genet.*, **14**, 269–276.
6. Sanpei, K., Takano, H., Igarashi, S., Sato, T., Oyake, M., Sasaki, H., Wakisaka, A., Tashiro, K., Ishida, Y., Ikeuchi, T. *et al.* (1996) Identification of the spinocerebellar ataxia type 2 gene using a direct identification of repeat expansion and cloning technique, DIRECT. *Nat. Genet.*, **14**, 277–284.
7. Imbert, G., Saudou, F., Yvert, G., Devys, D., Trottier, Y., Garnier, J.M., Weber, C., Mandel, J.L., Cancel, G., Abbas, N. *et al.* (1996) Cloning of the gene for spinocerebellar ataxia 2 reveals a locus with high sensitivity to expanded CAG/glutamine repeats. *Nat. Genet.*, **14**, 285–291.
8. Sobczak, K. and Krzyzosiak, W.J. (2004) Patterns of CAG repeat interruptions in *SCA1* and *SCA2* genes in relation to repeat instability. *Hum. Mutat.*, **24**, 236–247.
9. Choudhry, S., Mukerji, M., Srivastava, A.K., Jain, S. and Brahmachari, S.K. (2001) CAG repeat instability at *SCA2* locus: anchoring CAA interruptions and linked single nucleotide polymorphisms. *Hum. Mol. Genet.*, **10**, 2437–2446.
10. Reddy, P.S. and Housman, D.E. (1997) The complex pathology of trinucleotide repeats. *Curr. Opin. Cell Biol.*, **9**, 364–372.
11. Bates, G. (2003) Huntingtin aggregation and toxicity in Huntington's disease. *Lancet*, **361**, 1642–1644.
12. Michalik, A. and Van Broeckhoven, C. (2003) Pathogenesis of polyglutamine disorders: aggregation revisited. *Hum. Mol. Genet.*, **12**(Spec no. 2), R173–R186.
13. Cummings, C.J. and Zoghbi, H.Y. (2000) Fourteen and counting: unraveling trinucleotide repeat diseases. *Hum. Mol. Genet.*, **9**, 909–916.
14. Margolis, R.L. (2002) The spinocerebellar ataxias: order emerges from chaos. *Curr. Neurol. Neurosci. Rep.*, **2**, 447–456.
15. Stevanin, G., Durr, A. and Brice, A. (2002) Spinocerebellar ataxias caused by polyglutamine expansions. *Adv. Exp. Med. Biol.*, **516**, 47–77.
16. Li, S.H. and Li, X.J. (2004) Huntingtin and its role in neuronal degeneration. *Neuroscientist*, **10**, 467–475.
17. Heintz, N. and Zoghbi, H.Y. (2000) Insights from mouse models into the molecular basis of neurodegeneration. *Annu. Rev. Physiol.*, **62**, 779–802.
18. Koyano, S., Uchihara, T., Fujigasaki, H., Nakamura, A., Yagishita, S. and Iwabuchi, K. (1999) Neuronal intranuclear inclusions in spinocerebellar ataxia type 2: triple-labeling immunofluorescent study. *Neurosci. Lett.*, **273**, 117–120.
19. Huynh, D.P., Figueroa, K., Hoang, N. and Pulst, S.M. (2000) Nuclear localization or inclusion body formation of ataxin-2 are not necessary for *SCA2* pathogenesis in mouse or human. *Nat. Genet.*, **26**, 44–50.
20. Pang, J.T., Giunti, P., Chamberlain, S., An, S.F., Vitaliani, R., Scaravilli, T., Martinian, L., Wood, N.W., Scaravilli, F. and Ansorge, O. (2002) Neuronal intranuclear inclusions in *SCA2*: a genetic, morphological and immunohistochemical study of two cases. *Brain*, **125**, 656–663.
21. Huynh, D.P., Del Bigio, M.R., Ho, D.H. and Pulst, S.M. (1999) Expression of ataxin-2 in brains from normal individuals and patients with Alzheimer's disease and spinocerebellar ataxia 2. *Ann. Neurol.*, **45**, 232–241.
22. Huynh, D.P., Yang, H.T., Vakharia, H., Nguyen, D. and Pulst, S.M. (2003) Expansion of the polyQ repeat in ataxin-2 alters its Golgi localization, disrupts the Golgi complex and causes cell death. *Hum. Mol. Genet.*, **12**, 1485–1496.
23. Shibata, H., Huynh, D.P. and Pulst, S.M. (2000) A novel protein with RNA-binding motifs interacts with ataxin-2. *Hum. Mol. Genet.*, **9**, 1303–1313.
24. Nakahata, S. and Kawamoto, S. (2005) Tissue-dependent isoforms of mammalian Fox-1 homologs are associated with tissue-specific splicing activities. *Nucleic Acids Res.*, **33**, 2078–2089.
25. Ralser, M., Albrecht, M., Nonhoff, U., Lengauer, T., Lehrach, H. and Krobitsch, S. (2005) An integrative approach to gain insights into the cellular function of human ataxin-2. *J. Mol. Biol.*, **346**, 203–214.
26. Kedersha, N., Cho, M.R., Li, W., Yacono, P.W., Chen, S., Gilks, N., Golan, D.E. and Anderson, P. (2000) Dynamic shuttling of TIA-1 accompanies the recruitment of mRNA to mammalian stress granules. *J. Cell Biol.*, **151**, 1257–1268.
27. Kedersha, N. and Anderson, P. (2002) Stress granules: sites of mRNA triage that regulate mRNA stability and translatability. *Biochem. Soc. Trans.*, **30**, 963–969.
28. Giachino, C., Lantelme, E., Lanzetti, L., Saccone, S., Bella Valle, G. and Migone, N. (1997) A novel SH3-containing human gene family preferentially expressed in the central nervous system. *Genomics*, **41**, 427–434.
29. Harjes, P. and Wanker, E.E. (2003) The hunt for huntingtin function: interaction partners tell many different stories. *Trends Biochem. Sci.*, **28**, 425–433.
30. Cestra, G., Castagnoli, L., Dente, L., Minenkova, O., Petrelli, A., Migone, N., Hoffmuller, U., Schneider-Mergener, J. and Cesareni, G. (1999) The SH3 domains of endophilin and amphiphysin bind to the proline-rich region of synaptojanin 1 at distinct sites that display an unconventional binding specificity. *J. Biol. Chem.*, **274**, 32001–32007.
31. Sittler, A., Walter, S., Wedemeyer, N., Hasenbank, R., Scherzinger, E., Eickhoff, H., Bates, G.P., Lehrach, H. and Wanker, E.E. (1998) SH3GL3 associates with the Huntingtin exon 1 protein and promotes the formation of polygln-containing protein aggregates. *Mol. Cell*, **2**, 427–436.
32. Zarrinpar, A., Bhattacharyya, R.P. and Lim, W.A. (2003) The structure and function of proline recognition domains. *Sci. STKE*, **2003**, RE8.
33. Mayer, B.J. (2001) *SH3* domains: complexity in moderation. *J. Cell Sci.*, **114**, 1253–1263.
34. Nechiporuk, T., Huynh, D.P., Figueroa, K., Sahba, S., Nechiporuk, A. and Pulst, S.M. (1998) The mouse *SCA2* gene: cDNA sequence, alternative splicing and protein expression. *Hum. Mol. Genet.*, **7**, 1301–1309.
35. Albrecht, M., Golatta, M., Wullner, U. and Lengauer, T. (2004) Structural and functional analysis of ataxin-2 and ataxin-3. *Eur. J. Biochem.*, **271**, 3155–3170.
36. Dafforn, T.R. and Smith, C.J. (2004) Natively unfolded domains in endocytosis: hooks, lines and linkers. *EMBO Rep.*, **5**, 1046–1052.
37. Albrecht, M. and Lengauer, T. (2004) Survey on the PABC recognition motif PAM2. *Biochem. Biophys. Res. Commun.*, **316**, 129–138.
38. Ringstad, N., Nemoto, Y. and De Camilli, P. (2001) Differential expression of endophilin 1 and 2 dimers at central nervous system synapses. *J. Biol. Chem.*, **276**, 40424–40430.

39. Huntington's_Disease_Collaborative_Research_Group (1993) A novel gene containing a trinucleotide repeat that is expanded and unstable on Huntington's disease chromosomes. *Cell*, **72**, 971–983.

40. Ralser, M., Goehler, H., Wanker, E., Lehrach, H. and Krobitsch, S. (2005) Generation of a yeast two-hybrid strain suitable for competitive protein binding analysis. *Biotechniques*, **39**, 165–168.

41. Hughes, A.C., Errington, R., Fricker-Gates, R. and Jones, L. (2004) Endophilin A3 forms filamentous structures that colocalise with microtubules but not with actin filaments. *Brain Res. Mol. Brain Res.*, **128**, 182–192.

42. Micheva, K.D., Ramjaun, A.R., Kay, B.K. and McPherson, P.S. (1997) SH3 domain-dependent interactions of endophilin with amphiphysin. *FEBS Lett.*, **414**, 308–312.

43. Wu, J.Q., Bahler, J. and Pringle, J.R. (2001) Roles of a fimbrin and an alpha-actinin-like protein in fission yeast cell polarization and cytokinesis. *Mol. Biol. Cell.*, **12**, 1061–1077.

44. Landles, C. and Bates, G.P. (2004) Huntingtin and the molecular pathogenesis of Huntington's disease. Fourth in molecular medicine review series. *EMBO Rep.*, **5**, 958–963.

45. Reutens, A.T. and Begley, C.G. (2002) Endophilin-1: a multifunctional protein. *Int. J. Biochem. Cell Biol.*, **34**, 1173–1177.

46. Meriin, A.B., Zhang, X., Miliaras, N.B., Kazantsev, A., Chernoff, Y.O., McCaffery, J.M., Wendland, B. and Sherman, M.Y. (2003) Aggregation of expanded polyglutamine domain in yeast leads to defects in endocytosis. *Mol. Cell. Biol.*, **23**, 7554–7565.

47. Willingham, S., Outeiro, T.F., DeVit, M.J., Lindquist, S.L. and Muchowski, P.J. (2003) Yeast genes that enhance the toxicity of a mutant huntingtin fragment or alpha-synuclein. *Science*, **302**, 1769–1772.

48. Adams, A.E., Shen, W., Lin, C.S., Leavitt, J. and Matsudaira, P. (1995) Isoform-specific complementation of the yeast sac6 null mutation by human fimbrin. *Mol. Cell. Biol.*, **15**, 69–75.

49. Mumberg, D., Muller, R. and Funk, M. (1995) Yeast vectors for the controlled expression of heterologous proteins in different genetic backgrounds. *Gene*, **156**, 119–122.

50. Habermann, B. (2004) The BAR-domain family of proteins: a case of bending and binding? *EMBO Rep.*, **5**, 250–255.

51. Ringstad, N., Gad, H., Low, P., Di Paolo, G., Brodin, L., Shupliakov, O. and De Camilli, P. (1999) Endophilin/SH3p4 is required for the transition from early to late stages in clathrin-mediated synaptic vesicle endocytosis. *Neuron*, **24**, 143–154.

52. de Heuvel, E., Bell, A.W., Ramjaun, A.R., Wong, K., Sossin, W.S. and McPherson, P.S. (1997) Identification of the major synaptojanin-binding proteins in brain. *J. Biol. Chem.*, **272**, 8710–8716.

53. So, C.W., Caldas, C., Liu, M.M., Chen, S.J., Huang, Q.H., Gu, L.J., Sham, M.H., Wiedemann, L.M. and Chan, L.C. (1997) EEN encodes for a member of a new family of proteins containing an Src homology 3 domain and is the third gene located on chromosome *19p13* that fuses to MLL in human leukemia. *Proc. Natl Acad. Sci. USA*, **94**, 2563–2568.

54. Soubeyran, P., Kowanetz, K., Szymkiewicz, I., Langdon, W.Y. and Dikic, I. (2002) Cbl-CIN85-endophilin complex mediates ligand-induced downregulation of EGF receptors. *Nature*, **416**, 183–187.

55. Fabian-Fine, R., Verstreken, P., Hiesinger, P.R., Horne, J.A., Kostyleva, R., Zhou, Y., Bellen, H.J. and Meinertzhagen, I.A. (2003) Endophilin promotes a late step in endocytosis at glial invaginations in Drosophila photoreceptor terminals. *J. Neurosci.*, **23**, 10732–10744.

56. Ramjaun, A.R., Angers, A., Legendre-Guillemin, V., Tong, X.K. and McPherson, P.S. (2001) Endophilin regulates JNK activation through its interaction with the germinal center kinase-like kinase. *J. Biol. Chem.*, **276**, 28913–28919.

57. Cheung, N., So, C.W., Yam, J.W., So, C.K., Poon, R.Y., Jin, D.Y. and Chan, L.C. (2004) Subcellular localization of *EEN/endophilin A2*, a fusion partner gene in leukaemia. *Biochem. J.*, **383**, 27–35.

58. Qin, Z.H., Wang, Y., Sapp, E., Cuiffo, B., Wanker, E., Hayden, M.R., Kegel, K.B., Aronin, N. and DiFiglia, M. (2004) Huntingtin bodies sequester vesicle-associated proteins by a polyproline-dependent interaction. *J. Neurosci.*, **24**, 269–281.

59. Adams, A.E., Botstein, D. and Drubin, D.G. (1991) Requirement of yeast fimbrin for actin organization and morphogenesis *in vivo. Nature*, **354**, 404–408.

60. Drubin, D.G., Miller, K.G. and Botstein, D. (1988) Yeast actin-binding proteins: evidence for a role in morphogenesis. *J. Cell Biol.*, **107**, 2551–2561.

61. Karpova, T.S., Tatchell, K. and Cooper, J.A. (1995) Actin filaments in yeast are unstable in the absence of capping protein or fimbrin. *J. Cell Biol.*, **131**, 1483–1493.

62. Kubler, E. and Riezman, H. (1993) Actin and fimbrin are required for the internalization step of endocytosis in yeast. *EMBO J.*, **12**, 2855–2862.

63. Adam, T., Arpin, M., Prevost, M.C., Gounon, P. and Sansonetti, P.J. (1995) Cytoskeletal rearrangements and the functional role of T-plastin during entry of *Shigella flexneri* into HeLa cells. *J. Cell Biol.*, **129**, 367–381.

64. Delanote, V., Vandekerckhove, J. and Gettemans, J. (2005) Plastins: versatile modulators of actin organization in (patho)physiological cellular processes. *Acta Pharmacol. Sin.*, **26**, 769–779.

65. Delanote, V., Van Impe, K., De Corte, V., Bruyneel, E., Vetter, G., Boucherie, C., Mareel, M., Vandekerckhove, J., Friederich, E. and Gettemans, J. (2005) Molecular basis for dissimilar nuclear trafficking of the actin-bundling protein isoforms T- and L-plastin. *Traffic*, **6**, 335–345.

66. Giganti, A., Plastino, J., Janji, B., Van Troys, M., Lentz, D., Ampe, C., Sykes, C. and Friederich, E. (2005) Actin-filament cross-linking protein T-plastin increases Arp2/3-mediated actin-based movement. *J. Cell Sci.*, **118**, 1255–1265.

67. Lin, C.S., Park, T., Chen, Z.P. and Leavitt, J. (1993) Human plastin genes. Comparative gene structure, chromosome location, and differential expression in normal and neoplastic cells. *J. Biol. Chem.*, **268**, 2781–2792.

68. Matsudaira, P. (1991) Modular organization of actin crosslinking proteins. *Trends Biochem. Sci.*, **16**, 87–92.

69. Namba, Y., Ito, M., Zu, Y., Shigesada, K. and Maruyama, K. (1992) Human T cell L-plastin bundles actin filaments in a calcium-dependent manner. *J. Biochem. (Tokyo)*, **112**, 503–507.

70. Arpin, M., Friederich, E., Algrain, M., Vernel, F. and Louvard, D. (1994) Functional differences between L- and T-plastin isoforms. *J. Cell Biol.*, **127**, 1995–2008.

71. Satterfield, T.F., Jackson, S.M. and Pallanck, L.J. (2002) A Drosophila homolog of the polyglutamine disease gene *SCA2* is a dosage-sensitive regulator of actin filament formation. *Genetics*, **162**, 1687–1702.

72. Kondo, I. and Hamaguchi, H. (1985) Evidence for the close linkage between lymphocyte cytosol polypeptide with molecular weight of 64,000 (LCP1) and esterase D. *Am. J. Hum. Genet.*, **37**, 1106–1111.

73. Su, M.W., Dorocicz, I., Dragowska, W.H., Ho, V., Li, G., Voss, N., Gascoyne, R. and Zhou, Y. (2003) Aberrant expression of T-plastin in Sezary cells. *Cancer Res.*, **63**, 7122–7127.

74. Kari, L., Loboda, A., Nebozhyn, M., Rook, A.H., Vonderheid, E.C., Nichols, C., Virok, D., Chang, C., Horng, W.H., Johnston, J. *et al.* (2003) Classification and prediction of survival in patients with the leukemic phase of cutaneous T cell lymphoma. *J. Exp. Med.*, **197**, 1477–1488.

75. Sasaki, Y., Itoh, F., Kobayashi, T., Kikuchi, T., Suzuki, H., Toyota, M. and Imai, K. (2002) Increased expression of *T-fimbrin* gene after DNA damage in CHO cells and inactivation of *T-fimbrin* by CpG methylation in human colorectal cancer cells. *Int. J. Cancer*, **97**, 211–216.

76. Rao, R.M., Rama, S. and Rao, A.J. (2003) Changes in T-plastin expression with human trophoblast differentiation. *Reprod. Biomed. Online*, **7**, 235–242.

77. Sandrock, T.M., Brower, S.M., Toenjes, K.A. and Adams, A.E. (1999) Suppressor analysis of fimbrin (*Sac6p*) overexpression in yeast. *Genetics*, **151**, 1287–1297.

78. Nakano, K., Satoh, K., Morimatsu, A., Ohnuma, M. and Mabuchi, I. (2001) Interactions among a fimbrin, a capping protein, and an actin-depolymerizing factor in organization of the fission yeast actin cytoskeleton. *Mol. Biol. Cell.*, **12**, 3515–3526.

79. Ciechanover, A. and Brundin, P. (2003) The ubiquitin proteasome system in neurodegenerative diseases: sometimes the chicken, sometimes the egg. *Neuron*, **40**, 427–446.

80. La Spada, A.R. and Taylor, J.P. (2003) Polyglutamines placed into context. *Neuron*, **38**, 681–684.

81. Lebre, A.S., Jamot, L., Takahashi, J., Spassky, N., Leprince, C., Ravise, N., Zander, C., Fujigasaki, H., Kussel-Andermann, P., Duyckaerts, C. *et al.* (2001) Ataxin-7 interacts with a Cbl-associated protein that it recruits into neuronal intranuclear inclusions. *Hum. Mol. Genet.*, **10**, 1201–1213.

82. Faber, P.W., Barnes, G.T., Srinidhi, J., Chen, J., Gusella, J.F. and MacDonald, M.E. (1998) Huntingtin interacts with a family of WW domain proteins. *Hum. Mol. Genet.*, **7**, 1463–1474.

83. Kioka, N., Ueda, K. and Amachi, T. (2002) Vinexin, CAP/ponsin, ArgBP2: a novel adaptor protein family regulating cytoskeletal organization and signal transduction. *Cell Struct. Funct.*, **27**, 1–7.

84. Modregger, J., Schmidt, A.A., Ritter, B., Huttner, W.B. and Plomann, M. (2003) Characterization of Endophilin B1b, a brain-specific membrane-associated lysophosphatidic acid acyl transferase with properties distinct from endophilin A1. *J. Biol. Chem.*, **278**, 4160–4167.

85. Blagoev, B., Kratchmarova, I., Ong, S.E., Nielsen, M., Foster, L.J. and Mann, M. (2003) A proteomics strategy to elucidate functional protein–protein interactions applied to EGF signaling. *Nat. Biotechnol.*, **21**, 315–318.

86. Ho, Y., Gruhler, A., Heilbut, A., Bader, G.D., Moore, L., Adams, S.L., Millar, A., Taylor, P., Bennett, K., Boutilier, K. *et al.* (2002) Systematic identification of protein complexes in *Saccharomyces cerevisiae* by mass spectrometry. *Nature*, **415**, 180–183.

87. Wiedemeyer, R., Westermann, F., Wittke, I., Nowock, J. and Schwab, M. (2003) Ataxin-2 promotes apoptosis of human neuroblastoma cells. *Oncogene*, **22**, 401–411.

88. Schiestl, R.H. and Gietz, R.D. (1989) High efficiency transformation of intact yeast cells using single stranded nucleic acids as a carrier. *Curr. Genet.*, **16**, 339–346.

89. Puntervoll, P., Linding, R., Gemund, C., Chabanis-Davidson, S., Mattingsdal, M., Cameron, S., Martin, D.M., Ausiello, G., Brannetti, B., Costantini, A. *et al.* (2003) ELM server: A new resource for investigating short functional sites in modular eukaryotic proteins. *Nucleic Acids Res.*, **31**, 3625–3630.

90. Brannetti, B. and Helmer-Citterich, M. (2003) iSPOT: A web tool to infer the interaction specificity of families of protein modules. *Nucleic Acids Res.*, **31**, 3709–3711.

91. Obenauer, J.C., Cantley, L.C. and Yaffe, M.B. (2003) Scansite 2.0: Proteome-wide prediction of cell signaling interactions using short sequence motifs. *Nucleic Acids Res.*, **31**, 3635–3641.

92. Balakrishnan, R., Christie, K.R., Costanzo, M.C., Dolinski, K., Dwight, S.S., Engel, S.R., Fisk, D.G., Hirschman, J.E., Hong, E.L., Nash, R., Oughtred, R., Skrzypek, M., Theesfeld, C.L., Binkley, G., Lane, C., Schroeder, M., Sethuraman, A., Dong, S., Weng, S., Miyasato, S., Andrada, R., Botstein, D. and Cherry, J.M. (2005) *Saccharomyces Genome Database.* http://www.yeastgenome.org/.

93. Lin, C.S., Shen, W., Chen, Z.P., Tu, Y.H. and Matsudaira, P. (1994) Identification of I-plastin, a human fimbrin isoform expressed in intestine and kidney. *Mol. Cell. Biol.*, **14**, 2457–2467.